

An Investigation into the Sedimentary
laminations at West Basin Lake,
Victoria: Are they Varves?

Thesis submitted in accordance with the requirements of the University of
Adelaide for an Honours Degree in Geology

[Haimish Prodan]

November 2014



THE UNIVERSITY
of ADELAIDE

TITLE

An Investigation into the Sedimentary laminations at West Basin Lake, Victoria: Are they Varves?

RUNNING TITLE

Are West Basin Lake Sediments Varved?

ABSTRACT

West Basin Lake, in the Western Victorian Volcanic Region, has characteristics conducive to deposition of annually laminated sediments known as varves. The uppermost 50 cm of lake sediment consists of finely laminated, organic-carbonate sediments of a size and frequency that are typically associated with varved lake sediments. Varves hold tremendous potential as palaeoclimate indicators, allowing for the development of precise chronologies and annual scale climate reconstructions. Through detailed micro-facies analysis and counting of the West Basin lake sediments, the study found that the number of laminations was in good agreement with radiometric depth age modelling, suggesting annual deposition. It was concluded that although seasonal lamina were unable to be classified by the scope of this study, good agreement with radiometric depth-age modelling in conjunction with meromixis of West Basin Lake, its sheltered nature and sediment-water interface anoxia, suggest the laminations more likely represent varves than non-annual laminations and should warrant further investigation.

KEYWORDS

Varves, West Basin Lake, Carbonates, Organic rich, Annual laminations, Meromixis, Anoxia, Laminated sediment

TABLE OF CONTENTS

Title..... i
Running title i
Abstract..... i
Keywords..... i
List of Figures and Tables 2
INTRODUCTION 7
METHODS 11
Coring and Storage 11
Subsampling 11
Resin Embedding..... 13
Thin Section Microscopy 14
Scanning Electron Microscope (SEM) 14
Lamination Counting 14
RESULTS: OBSERVATIONS AND INTERPRETATIONS 14
Petrography of Sediment Constituents 15
Carbonates 15
Organic Matter..... 15
Allogenic, Other and Unidentified Material 16
Diagenesis..... 18
Laminations 19
Dark vs Light 19
Carbonate Rich Laminations 20
Organic Rich Laminations..... 21
Lamination Counts 21
Depth – Age Relationship 24
Scanning electron microscope (SEM) Micro-facies Analysis..... 36
Low Vacuum SEM using soft sediment 36
Environmental SEM (ESEM) using soft sediment..... 36
High Vacuum SEM using resin embedded sediments 37
Down-core variability in Sediment Composition..... 39
DISCUSSION..... 39
Are the Laminations Varves? 39
Potential for Varve Deposition 40

Carbonate vs. Organic Deposition.....	42
Potential for Varve Preservation.....	43
West Basin Meromixis and Anoxia.....	43
Why not Varves?	44
Depth-Age Relationship	45
Future Direction.....	47
SEM (what else can this provide?).....	47
LA-ICP-MS	48
Dating	48
Sediment Trap Studies.....	49
CONCLUSIONS	49
Acknowledgments	50
References	50
Appendix A: Extended methods, Resin Recipe & Misc.	53

LIST OF FIGURES AND TABLES

Figure 1: Location map of the study area. (d) Lake bathymetry and surrounding topography adapted from Gell et al. (1994).	10
Figure 2: Showing the aluminium boxes which have been embedded into the sediment core	12
Figure 3: Showing the desiccation apparatus with which a vacuum pump was attached to facilitate impregnation of the resin into the samples. The yellow fluid is the Spurr's resin.	12
Figure 4: Reflected light micrograph image showing what is likely an authigenic pyrite framboid which was growing within a spore. Width of image = 174 um.	18
Figure 5: (a) Shows lamination thickness variation through time and an increasing lamination thickness towards present day. This plot does not display thicknesses of zones where laminations appeared absent and hence, splices the laminated zones as a continuous chronology (i.e. the 621st lamination is likely older than 621 years). Thus, is only here to show the trend that lamination widths decrease with age. (b) Shows lamination frequency variation with depth and an increase in lamination frequency per 2 cm with depth. The widths of the laminations have been corrected for shrinkage and represent true widths in both plots.....	23
Figure 6: A reproduction of the top of the depth-age model for West Basin Lake adapted from Gell et al. (1994). The shape of the curve is a smooth spline. The green data represent six independent Pb210 ages and the blue data represents the earliest of three ¹⁴ C radiocarbon age probability density histograms produced from West Basin Lake (Last and De Deckker 1990). The grey band represents the 95% confidence interval. The series of data points (black, open pinpoints) represents the cumulative	

number of laminations per 2 cm of West Basin Lake sediment. 0 cal BP = 1986. The horizontal and vertical lines intersect at 50 cm depth and 621 cal BP respectively..... 25

Figure 7: Photomicrographs of some of the common constituents of the calcareous component of West Basin Lake sediments. (a) A typical sub-rounded, sub-spherical peloid of microcrystalline carbonates (micrite) also exhibiting a cloudiness which is not uncommon (PPL). (b) A similar peloid viewed under XPL displaying third order creamy birefringent colours. It also appears to have some organic matter, most obvious in the centre, and probably accounts for the slight brown colouration. (c) A peloid viewed under XPL with the λ 530 nm tint plate inserted, displaying third order birefringent colours giving an overall creamy green appearance. (d) A mineral commonly seen disseminated throughout the profile. Its relief changed upon stage rotation, a common property of carbonate minerals. The brown colouration could be a staining by organic matter, or may be the Fe bearing carbonate, siderite. (e) The same mineral grain viewed under XPL displaying first order orange/yellow birefringent colours. (f) A peloid/intraclast of unknown composition, potentially fecal in origin, sitting in a carbonate rich matrix. Its optical properties were not vastly different between PPL and XPL and may indicate an organic composition represented by the opaque material within it. A thin micritic envelope can also be seen around the grain. (g) A small cluster of acicular, colourless-grey minerals (potentially aragonite or needle-calcite) in an organic rich matrix. Relief changes were observed upon rotation of the stage and exhibited third order creamy birefringence colours under XPL. This crystal habit of carbonates or at least a clustering of them was a rare occurrence. (h) A small cluster of well-articulated ostracod valves in a carbonate rich matrix (XPL). They commonly exhibit a sweeping extinction in XPL (i) A peloid/intraclast of micrite viewed under XPL. Notice the inclusion to the left of centre of the clast which appears to truncate at the grain boundary. This might indicate the clast was already lithified and may originate from the nearshore hardgrounds of the lake. The light brown colouration of the clast and surrounding carbonate matrix probably indicates organic matter is also present..... 27

Figure 8: Photomicrographs of some of the common constituents of the organic component of West Basin Lake sediments. All images were acquired in PPL. (a) An organic particle of what may be a pollen spore or other plant component. It appears to have cellular structure. (b) A particle of amorphous organic matter. There is an associated pore space (colourless) which may have once been occupied by more matter which has since disintegrated. (c) A common, more tabular, elongate and larger particle of organic matter. Smaller particles of opaque amorphous organic matter can be seen speckled through the surrounding carbonate matrix. (d) The brown, triangular shaped particle in the centre is an example of another common particle of organic matter which appears translucent and brown - reddish brown in PPL but becomes opaque in XPL. Cellular structure is clearly evident. (e) A transverse image of what might be a vegetative stem. Cellular structure is strikingly prominent. (f) A very common component throughout the sediment. They are morphologically consistent and are likely to be pollen spores. (g) This image captures an organic rich zone, recognisable by the dark brown sediment and disseminated, black amorphous organic matter throughout. The ~ 200 μ m sized particle slightly left of centre, may represent another transverse through a vegetative stem. Although it is not easily visible at this scale, at higher magnifications, cell walls can be discerned. Another more reddish-brown cellular body can be seen toward the top right of the image. (h) An overview of a zone where the

largest organic and cellular, likely vegetative tissues have been deposited. (i) A large amorphous particle of organic matter in a carbonate and organic mixed matrix. This may also represent a particle of charcoal..... 29

Figure 9: Photomicrographs showing some of the non-carbonate minerals and the nature of grain coatings of West Basin Lake sediments. (a) A mineral grain with the development of a cement coating exhibiting similar third order birefringent orange - yellow colours as the grain in Figure 7 (e). It is not a micritic coating. (b) A mineral grain with a micritic envelope. The micritic envelopes often appear dark – nearly opaque, and hazy. The surrounding matrix is rich in carbonates (note the hazy grey appearance). (c) An XPL image showing a grain exhibiting very low first order yellow birefringence, verging on opaque with an asymmetrical envelope of micrite. (d) A PPL image potentially of the remains of a gastropod. Chambers have been filled with micrite and opaque material which may be organic. In the left most chamber, you can notice a segmentation type pattern in the calcareous wall. Blocky calcite appears to be replacing the original wall of the upper right chamber. A micritic envelope can be seen. (e) An XPL image showing a ghost grain with a rare example of a coating which is not micritic but is most likely calcitic or dolomitic. The original grain appears to have dissolved and micrite has begun filling in the space. (f) An XPL image of a quartz grain with an envelope of micrite. (g) A PPL image of a translucent clast containing smaller grains of quartz. (h) An XPL image of (h). The clast shows a mottled colouration and looks as though it may have undergone some chemical alteration. It may have originated from the nearshore hardgrounds of the lake. (i) An XPL image of a small grain of feldspar, exhibiting multiple twinning. The surrounding carbonate matrix has a brown colouration possibly attributable to the presence of organic matter..... 31

Figure 10: Photomicrographs showing some of the diagenetic mineral precipitation of West basin Lake sediments. (a) A PPI image showing blocky carbonate crystals (likely calcite or dolomite) growing from one half of an ostracod valve. (b) An XPL image of an originally well-articulated ostracod valve appearing to have been replaced by microcrystalline carbonate crystals (calcite or dolomite). The fabric appears fibrous where the two valves meet. (c) A similar XPL image to (b) showing ostracod valves and fragments being replaced by microcrystalline carbonates. (d) An XPL image of vegetative tissue where the cellular structures have been replaced by calcareous cement. (e) An XPL image of more ostracods being replaced by microcrystalline carbonates. Notice the pore space has nearly been completely filled in the top-centre ostracods. The sweeping, cross-extinction can be seen, especially in the above centre ostracod. (f) An apparent growth of calcite forming around an unidentified nucleus (g) A PPL image showing two mineral grains with incomplete coatings of dark reddish-brown cement. Note how it cuts through the lowermost grain. Some relief change was noted in the crystals of the cement in the lowermost grain upon rotation of the stage, indicating it could be a carbonate (siderite). (h) An XPL image of (g). The central grain has a micritic envelope as well as the lowermost grain..... 33

Figure 11: Photomicrographs showing the general characteristics of the laminations in West basin Lake sediments. The top of the core is to the left in all images. (a) A PPL image showing one of the lightest, slightly yellow laminations running sub-vertically through the centre. Fenestral type porosity can also be seen in the zones adjacent to the lamination. The adjacent sediment is also quite peloidal. The surrounding sediment either side is carbonate rich. It may have been a microbial mat which has since been removed and filled with resin. (b) A PPL image showing a thick carbonate lamination

also rich in organics, attributing the brown colour. Note the grading of coarser carbonate minerals at the base (right) into finer, more micritic, darker and denser sediment into the top (left). (c) An XPL image of (b) where the difference in coarseness can be more clearly noted. Also note the cloudy appearance of the lamination, characteristic of carbonate rich components. (d – f) Image series of organic rich laminations in PPL, XPL and XPL with the λ 530 nm tint plate inserted respectively. Notice how under XPL, without the tint plate (e), the laminations become much harder to distinguish as organic content remains opaque or becomes darker, creating the illusion of a homogenous sediment. Even the abundant clastics and non-carbonate grains are homogeneously disseminated throughout. The darkest lamina is likely to be the richest in organics, whilst the lightest, slightly yellow appear sparse in any type of component and has mostly become occupied with resin. Notice that there appears to be a repetitive and cyclic deposition. (g – i) Image series of alternating carbonate and organic rich laminations taken under PPL, XPL and XPL + tint plate respectively. Note how the sediment appears nearly homogeneously coloured and composite under PPL (g) but under XPL, without and with the tint plate inserted (h and i respectively), compositionally contrasting laminations are revealed. The XPL image (h) reveals a carbonate rich lamination in the centre, bracketed by darker, nearly opaque organic rich laminations either side. The XPL + tint plate image (i) showcases the diagnostic third order creamy green birefringence of carbonate rich lamina. Note how there is little change in the organic matter between PPL and XPL + tint plate, but sometimes appearing with orange hues as seen in (i)..... 35

Figure 12: A series of backscatter electron micrographs acquired using ESEM mode, imaging a ~ 50 x 50 x 50 mm cube of raw, wet West Basin Lake sediment extracted between 100 – 110 mm depth from the core. (a) Shows what is likely the surface of an ostracod shell - notice the porous texture. (b) Notice in the top of the image, an amorphous wavy, folded, slightly darker looking particle embedded in the matrix which is likely organic matter. (c) A good representation of the fineness of the carbonate and clay sized non-carbonate grains (bright white particles) embedded in what is probably an organic matrix (darker and grey). (d) Notice the larger, clumpy grains which probably reflect the peloid grains commonly observed in thin section of carbonate rich lamina. 37

Figure 13: A series of backscatter electron micrographs acquired using high vacuum mode imaging various solid, resin embedded West Basin Lake samples. The top of the core is to the left in all images (a) Notice the abundance of peloidal grains constituting much of the sediment. There is a good degree of intergranular porosity amongst the peloids where dark grey resin has infiltrated. Several ostracods can also be seen and the voids within them have been infiltrated by resin. The more anhedral, broken up bright grains in the right portion of the image are likely to be carbonates and/or purely micritic peloids whereas the more euhedral grains are more likely non-carbonates such as quartz and other silicates. (b) The matrix here is much more dense and homogenised and peloids cannot be recognised. A lamination running vertically, slightly left of centre and is abundant with carbonate and various detrital grains can be distinguished. Two ostracod valves can be seen in the right portion of the image. Some dark grey material is speckled throughout and probably represents organic matter and/or potentially pore space. (c) A thin lamination running vertically through the centre of apparently homogenous looking sediment can be distinguished. It is likely richer in carbonates and/or silicates than the adjacent sediment either side. (d) Notice the large pore spaces

which appear to have been completely infiltrated with resin actually also contain large, cellular plant tissue which can no longer be discerned. 38

Figure 14: The uppermost plot shows mean monthly maximum temperature during the period 1899 – 1983 for the Colac region, Victoria. The lower plot shows mean monthly rainfall during the period 1898 – 2014 for the Colac region, Victoria..... 41

Figure 15: The 70 – 140 mm carbonate rich zone where laminations appear absent/on hiatus..... 46

Table 1: The subsamples collected from each core half. One subsample was 1 cm longer than the other. WB; West Basin, N; North half, S; South half 13

INTRODUCTION

One of the biggest challenges presently faced is the ability to quantify climate change and to understand the role humans have played and will continue to play in the future of global climate. To determine how climate may behave in the future, we need to understand how it did so in the past. Australian climate is naturally intra- and inter-annually variable with sporadic sub-annual events (e.g. the extreme rains which resulted in the 2011 Queensland floods (Boening et al. 2012)). Mainland Australia is surrounded by ocean where on-shore climate is co-dependently driven by the Indian Ocean Dipole, the Southern Annular Mode and the El Nino Southern Oscillation (IOD, SAM and ENSO respectively (Ummenhofer et al. 2009, Neukom and Gergis 2012)). However, archives resolving high and low frequency climate variability over long timescales (especially during the Holocene) in Australia and the southern hemisphere overall, are not extensive or have not yet been discovered (Neukom and Gergis 2012). This becomes an issue because unless highly resolved temporal archives are used, important features of the climate system, in particular the long term nature of critical inter-annual climate features (e.g. ENSO) remains poorly understood.

Previous research in the southern hemisphere has attempted to capture high and low frequency climate variability and environmental change. In Australia, fossil diatoms have been used to reconstruct the last 1500 years of climate variability (Barr et al. 2014). Other climate research has investigated pollen, carbon/nitrogen, macrofossil and ostracods for palaeoclimate and environmental reconstructions (Gouramanis et al. 2010, Barr et al. 2013). Tree ring analysis of *Agathis australis* from New Zealand provided a 423 year high resolution record of ENSO variability (Fowler 2008). However, tree ring

records are typically developed from younger and living trees in the southern hemisphere and generally only cover the last 500 years, as living trees which extend farther back in time are few (Neukom and Gergis 2012). A rare exception is the 3000 year long Huon Pine tree ring record from Mt. Read, Tasmania (Cook et al. 2000). Like tree rings, corals are also useful for extracting high resolution (annual) data (Bagnato et al. 2004) but the genus *Porites* which is commonly used for paleoclimatic studies in the southern hemisphere, does not typically extend past 300 – 400 years (Neukom and Gergis 2012).

The potential for highly resolved and precisely dated, temporally extensive climate and environmental reconstructions, capturing high - low frequency climate variability, can lie within varves (annual and repetitive laminations); theoretically representing one year of sediment deposition. The potential for varve chronologies as robust archives of climate variability has been demonstrated at a number of locations, across a wide range of climate scenarios e.g. Lake Van, Turkey (Landmann et al. 1996), Elk Lake, United States (Bradbury and Dean 1993), Lake C2, Arctic Canada (Lamoureux and Bradley 1996), Lake Suigetsu, Japan (Kitagawa and van der Plicht 1998) and Lake Bosumtwi, Ghana (Shanahan et al. 2008). To date, no Holocene varved records have been reported from Australia, despite considerable potential and a definite need.

A number of lakes in the Western Victorian Volcanic Region contain finely laminated sediments, with particular interest in the finely laminated carbonate rich sediment from West Basin Lake, Victoria (Figure 1). These sediments span at least the last 10, 000 years (Last and De Deckker 1990, Gell et al. 1994) and are situated in a region which is

influenced by a range of high and low frequency climate signals (IOD, SAM, ENSO and IPO).

Before laminated sediments can be interpreted as varves and used to construct climate variability at annual resolution, a detailed assessment is required of the sedimentology of those laminae, and an independent test of their frequency of deposition. This paper explores this potential using transmission and reflective optical light microscopy and scanning electron microscope (SEM). The aim is to: (a) assess the depositional nature of laminated sediments at West Basin; (b) provide a petrographic basis for the qualitative interpretation of high resolution geochemical data; and (c) conceptually and empirically evaluate the hypothesis that the laminations at West Basin are annually deposited – i.e. that they are varves. If the varve hypothesis is supported, a varve record from West Basin would provide a basis for reconstructing a year-to-year, precise record of high and low frequency climate variability. These data would provide new insights into the large scale drivers of southeast Australian climate and may help to predict the next ‘Big Dry.’

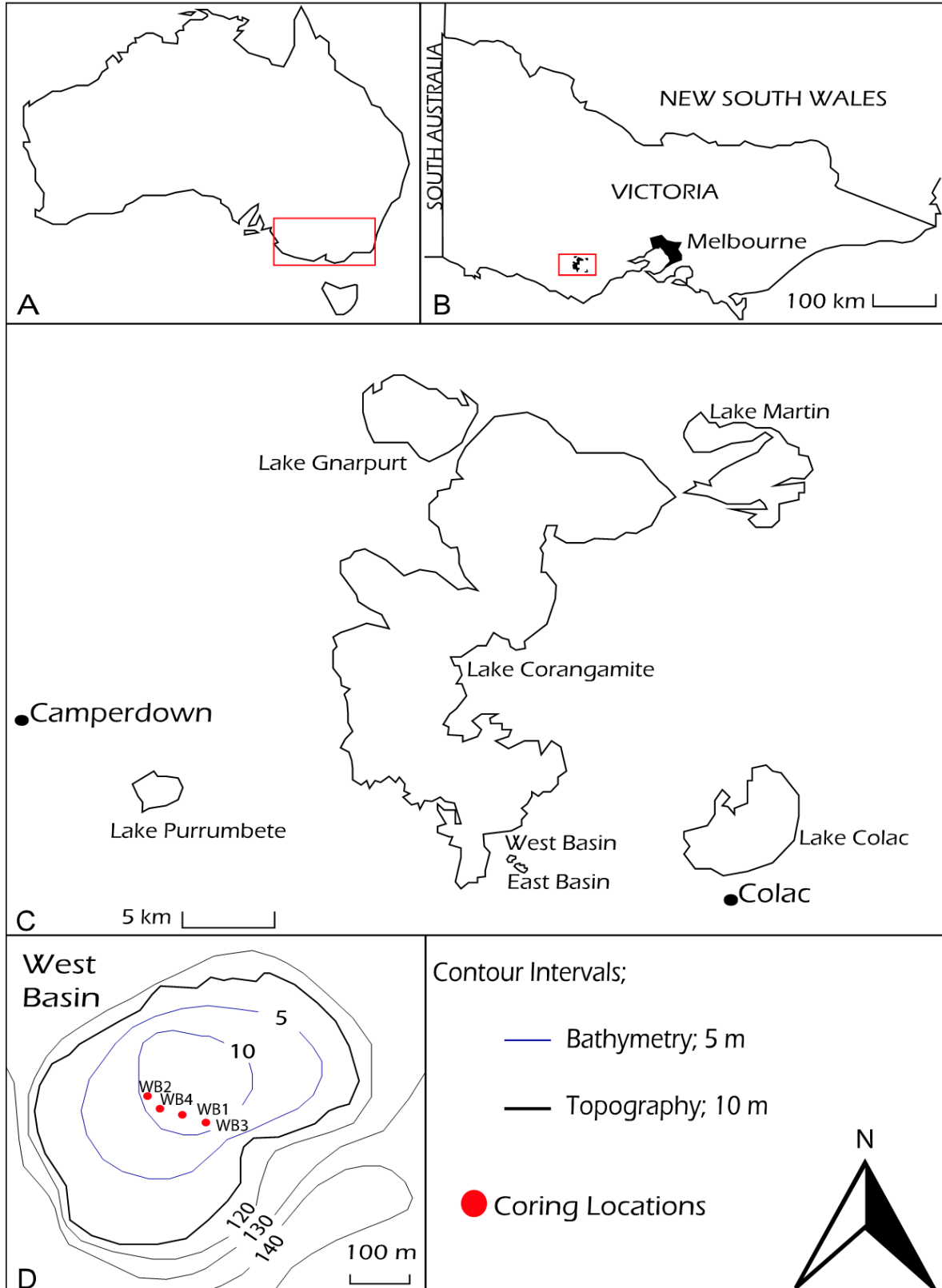


Figure 1: Location map of the study area. (d) Lake bathymetry and surrounding topography adapted from Gell et al. (1994).

METHODS

For the extended and detailed methodology, refer to Appendix A.

Coring and Storage

Sediment coring was carried out in 1986 using a Mackereth corer, with cores subsequently sealed and stored at 4° C at the Australian National University until 2013 (Last and De Deckker 1990).

Subsampling

Subsampling was carried out using handmade rectangular boxes of 0.1mm aluminium foil with dimensions 70 x 12 x 10 cm (Figure 2). Twenty subsamples in total (10 x (70 x 12 x 10 mm) and 10 x (~ 50 x 50 mm cubes); Table 1) were extracted from the 0-1 m West Basin core. The samples remained sealed within cling film and refrigerated (1-4°C), to prevent desiccation, until required.

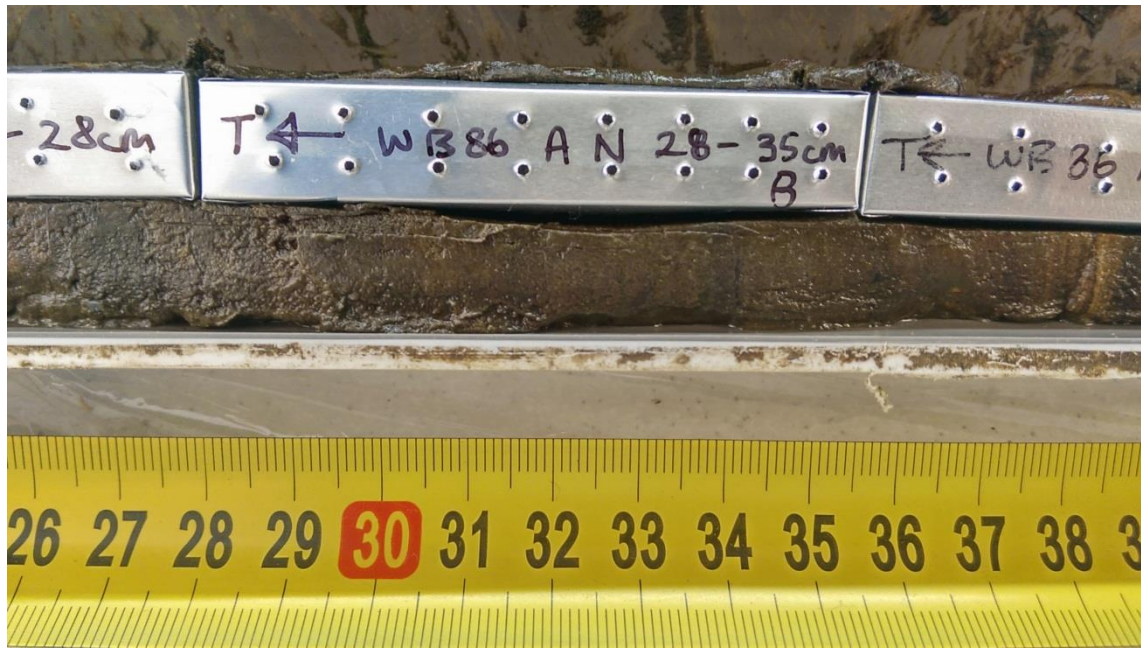


Figure 2: Showing the aluminium boxes which have been embedded into the sediment core

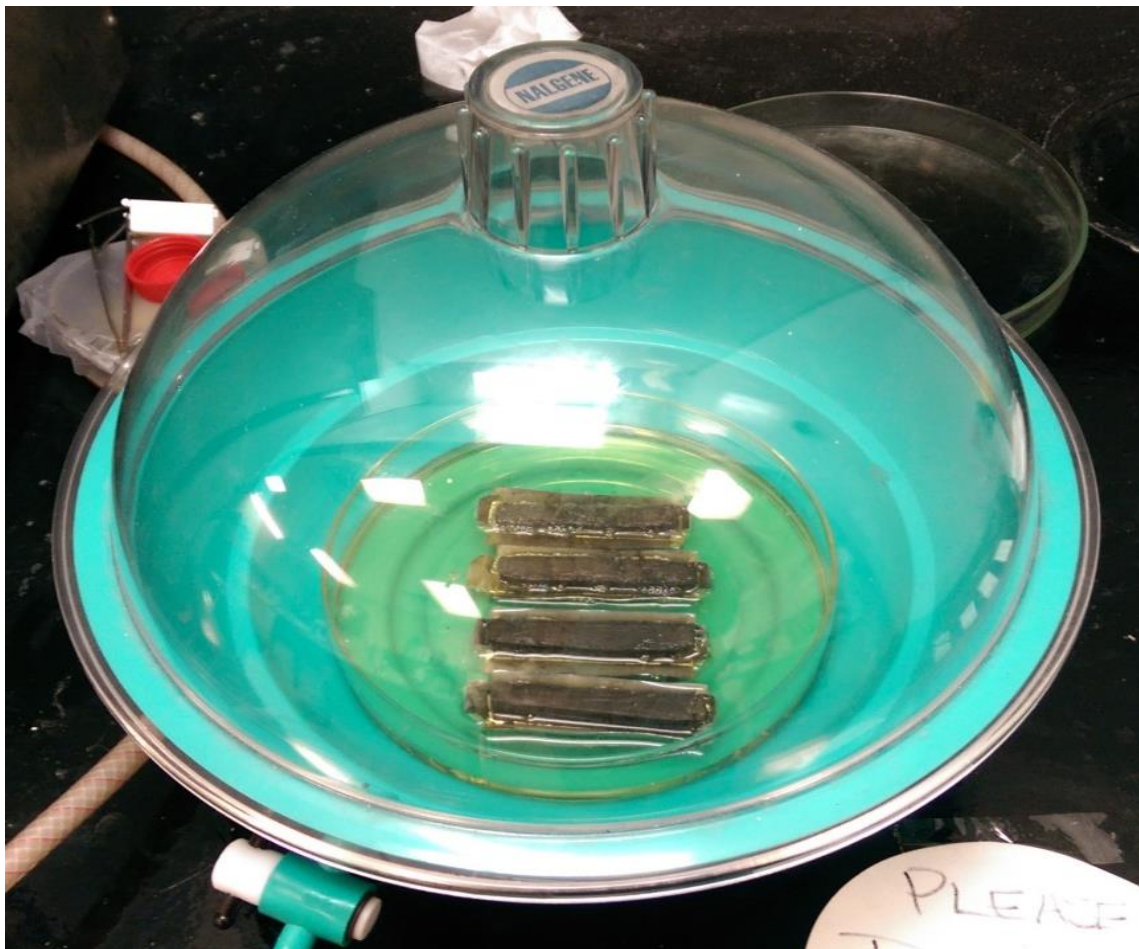


Figure 3: Showing the desiccation apparatus with which a vacuum pump was attached to facilitate impregnation of the resin into the samples. The yellow fluid is the Spurr's resin.

Core Halves				Subsamples (mm)			
WB86 A N (0-1 m)	0-70	70-140	140-210	210-280	280-350	350-420	420-500
WB86 A S (0-1 m)	150-220	220-290	290-370				

Table 1: The subsamples collected from each core half. One subsample was 1 cm longer than the other. WB; West Basin, N; North half, S; South half

Resin Embedding

A number of different approaches have been described for the resin impregnation of lake sediments (Lamoureux 1994, Pike and Kemp 1996, Lotter and Lemcke 1999). The acetone-epoxy exchange procedure, adapted from Lotter and Lemcke (1999) was implemented to embed the sediments for this study.

The sediments were laid in a large glass petri dish and well submerged in acetone – water solutions of gradually increasing strength, starting at a 50:50 acetone-water solution and graded up to 100% acetone over six exchanges. They were left to soak for at least 24 hours for each exchange. Once the acetone had completely replaced the pore water, resin was introduced as a 50:50 acetone-resin mixture and graded up to 100% resin over four 24 hour exchanges. Each resin-acetone exchange was carried out in a desiccation chamber under low vacuum (Figure 3). After the final 100% resin exchange, the samples were cured as blocks in an oven for 24 hours at 70°C. Once the samples had hardened, they were cut down into smaller blocks and then cut in half so that a surface of the sediment was exposed.

Thin Section Microscopy

Ten thin sections were manufactured by Pontifex & Associates Pty Ltd. They were analysed using a Nikon LVL 100 POL transmission and reflected light optical microscope.

Scanning Electron Microscope (SEM)

Scanning Electron Microscope was carried out under high and low vacuum, as well as using Environmental SEM (ESEM) mode. Low vacuum SEM and ESEM was carried out using untreated sediment blocks, whereas high vacuum SEM was carried out using resin embedded sediments. Backscatter electron (BSE) images were predominantly produced rather than secondary electron (SE) images. Transects were imaged along the length (perpendicular to laminations) of the three stratigraphically uppermost 70 x 12 x 10 mm samples.

Lamination Counting

Transect style micrographs were imaged of seven stratigraphically consecutive WB86 A N sample thin sections (Table 1). The images were stitched using Microsoft ICE (freeware) and imported into ImageJ (freeware) to count laminations and measure widths.

RESULTS: OBSERVATIONS AND INTERPRETATIONS

Due to the high water content of the sediments, resin embedding the samples had resulted in about ~ 14% shrinkage across the seven WB86 A N samples which were petrographically analysed. Any depths or widths of laminations which are referred to in

the results are the measurements recorded from the thin section samples, rather than the corrected true depth or width measurements unless otherwise stated.

Petrography of Sediment Constituents

CARBONATES

Carbonates made up a significant proportion of the lake sediments and were at least sparsely disseminated throughout organic rich laminations or zones. Carbonate minerals predominantly consisted of clay to silt sized (2 – 5 μm) subhedral grains which were likely calcite and dolomite. Less frequently, some grains had an elongated, tabular or acicular morphology and were likely to be aragonite.

Sub-angular to sub-rounded peloidal and intraclastic grains of micrite and calcareous material were also very common throughout the sediment profile, though were mostly concentrated and largest in carbonate rich laminations (Figure 7; a – g and i). They ranged in size from 35 – 300 μm (averaging ~ 90 μm).

Calcitic ostracods and skeletal fragments (derived from ostracods) also comprised much of the carbonates in the sediment and are abundantly disseminated throughout (Figure 7 h).

ORGANIC MATTER

Organic matter also made up a significant but lesser portion of the sediment. However due to resin impregnation, it was difficult to determine the nature of much of the organic constituents, bar those very coarse fragments such as plant matter and charcoal.

Visible organic matter included materials which were almost certainly plant detritus and charcoal (see Figure 8 a – i).

In plane polarised light (PPL) it mostly appeared black/opaque and/or light shades of brown and slightly translucent (Figure 8 a – i). Organic constituents could be distinguished from minerals because their shapes were often irregular and anhedral (amorphous), lacked any signs of cleavage and their optical properties (e.g. birefringence, extinction) did not change between PPL, cross polarised light (XPL) and rotations of the stage (e.g. relief and pleochroism). The only exception was if the organic matter was translucent, it always became opaque in XPL but went translucent again when the tint plate was inserted. Visible organic constituents were predominantly amorphous (Figure 8 b) but other common morphologies included tabular, elongated, spherical and fibrous shapes (Figure 8; a, c & f). The visible organic matter had a broad size range covering 18 μm – 10 mm (averaged ~ 85 μm).

ALLOGENIC, OTHER AND UNIDENTIFIED MATERIAL

Allogenic or detrital components (excluding visible organic matter) averaged ~60 μm and encompassed very minor amounts of the total 490 mm sediment profile (~15%). They were commonly disseminated throughout the sedimentary profile and abundances varied with depth. Occasionally detrital material could be seen more or less laterally concentrated as fine lamina; potentially reflecting an event deposit (Figure 13 b). This was only observed several times and usually in zones where detrital material was almost absent or much less abundant in the sediment.

The predominant and highest occurring detrital grain and most easily identifiable was quartz (Figure 9; a, b, f & g – i). The remainder of the material was not easily identifiable (except for several grains of feldspar) but probably consisted of clay minerals, silicates, skeletal remains and potentially extraclasts from the nearshore hardgrounds at the perimeters of the lake (Figure 9; c, d & e). A framboid of pyrite was seen formed within what appeared to be a pollen spore (Figure 4).

Another particularly common grain was one which appeared a translucent brown/amber colour (PPL), consistently subhedral and sometimes looked mottled or pitted as though it had been chemically altered (enhanced by XPL (Figure 9 g & h). In XPL, they usually exhibited a first order orange/amber or yellow birefringence. They sometimes contained inclusions of detrital quartz or other grains and therefore may be clasts of lithified cement/sediment from the nearshore hardgrounds (Figure 9 g & h).

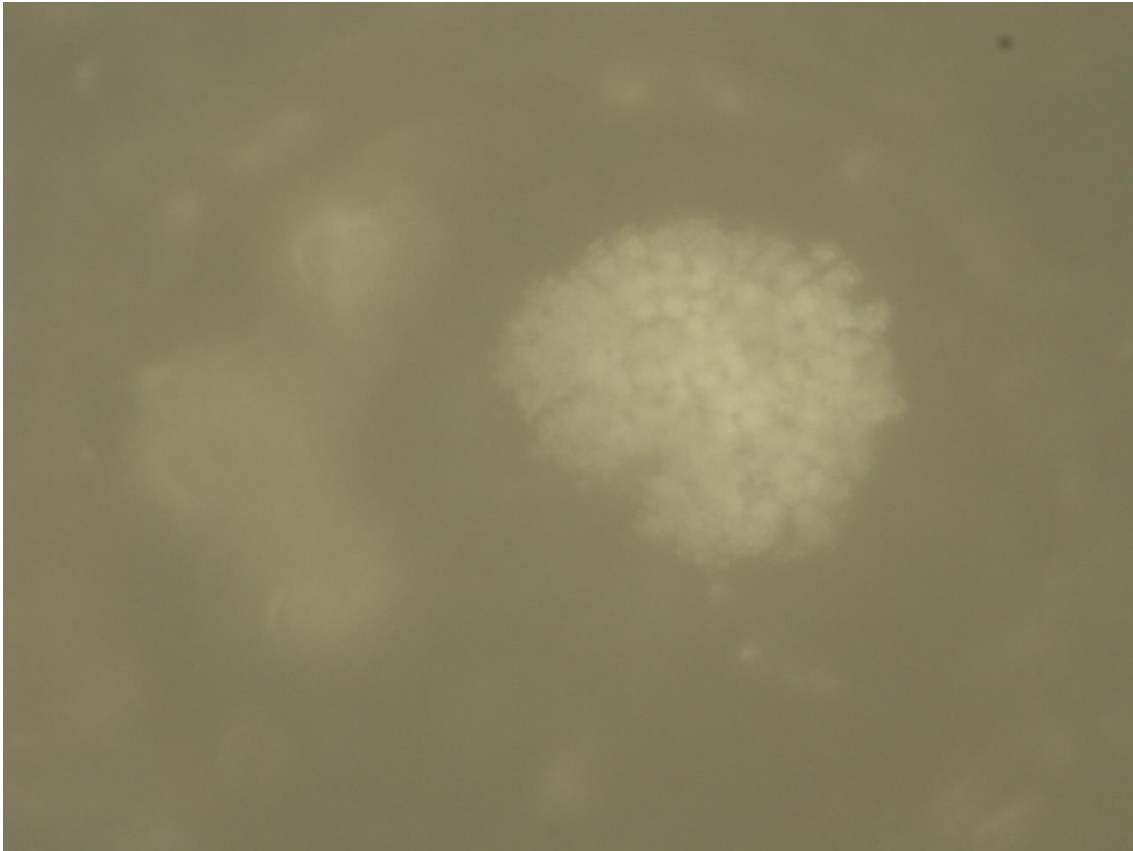


Figure 4: Reflected light micrograph image showing what is likely an authigenic pyrite framboid which was growing within a spore. Width of image = 174 μ m.

DIAGENESIS

Evidence of diagenesis and secondary carbonate precipitation was not an uncommon feature throughout the sediment profile despite being recent. The most common secondary precipitation phenomena observed was neomorphism of ostracod valves and skeletal fragments (Figure 10; a – c & e). The original calcitic ostracod valves became replaced by finer crystalline carbonates which also began filling in the void space (Figure 10; b, c & e). The crystal fabric often grew in optical continuity with the ostracod valve and commonly exhibited a sweeping extinction under XPL (Figure 10 e). Less frequently, blocky carbonate minerals could sometimes be seen as a secondary precipitate nucleating from ostracod valves (Figure 10 a).

LAMINATIONS

The top 490 mm of West Basin Lake offshore sediment was dominated by finely laminated organic rich carbonate mud. The laminations were predominantly diffuse and boundaries were rarely sharp. The laminations averaged 780 µm thick and were primarily defined by contrasts in colour and to lesser degrees, texture and/or grain size. A total of 621 laminations were counted for the 490 mm profile.

Dark vs Light

The colour variations observed in thin section (PPL) were shades of brown/tan, yellow and grey (Figure 11; a, b, d & g). There were some compositional variances between different coloured lamina but there was seldom a sharp distinction between pure carbonate vs organic scenarios. Transitions between most adjacent laminations primarily differed according to the amounts of fine scale carbonates in proportion to amounts of organic matter and vice versa.

The largest degree of colour variation was exhibited between the organic rich laminations (Figure 11 d). The cause of this colour variation between presumably similar lamina was much less obvious and irresolvable by optical microscopy alone. Generally, the darker the lamination (PPL and XPL) the richer it was likely to be in organic matter. This was supported by the fact that darker laminations are often sparse in carbonates and allogenic material (excluding detrital plant matter). However some dark laminations were actually rich in carbonates and appeared similar to dark laminations rich in organic matter (Figure 11; b, c & g – i), but upon closer investigation, the differences became apparent.

Carbonate Rich Laminations

Under plane polarised light (PPL), carbonate rich laminations had a dirty/dusty grey appearance and commonly appeared speckled with sub-angular to sub-rounded grey and/or brown peloids/intraclasts of micrite (calcareous grains < 5 μm) or reworked carbonate mud. When viewed under cross polarised light (XPL) and lower magnifications (25x), the lamina exhibited overall first order creamy white/grey birefringent colours. When a λ 530 nm sensitive tint plate was inserted under XPL, the carbonate rich lamina could be much more easily identified (Figure 11 h & i). At similar low magnifications they produced an overall third order, pale, creamy, sometimes dark, green birefringence (Figure 11 i). More often than not however, these carbonate laminations usually appeared a dusty brown rather than grey in PPL (Figure 11 b & g). The brown colouration of the carbonates is likely attributable to incorporation with organic matter.

The majority of dark laminations however, were varying mixtures of carbonate and non-carbonate constituents (primarily microscopic organic matter). It was therefore important to observe all laminations comparatively under PPL and XPL, with and without the tint plate. This avoided accidental misclassification between organic rich lamina and carbonate lamina contaminated with microscopic organic matter, which both appeared similarly brown. Regardless, carbonate rich laminations, contaminated with organics or not, only differed significantly by their colour in PPL (brown = organic contamination; grey = organic poor).

Organic Rich Laminations

Under PPL, organic rich laminations appeared varying shades of brown, tan and sometimes yellow (Figure 11 d & g). They were usually fine and did not have the dirty/dusty appearance or peloidal grains such as those rich with carbonates. Oddly, they were seldom richer in visible organic matter but several cases were seen where this was not the case.

Viewing with XPL did not deliver significant optical contrasts from PPL. All visible organic matter would turn opaque and an organic rich lamination or zone generally became darker, especially if it was deficient in carbonates. When viewing with the tint plate inserted, the optical properties remain the same as that of PPL except some of the lighter hues (tans and yellows) become slightly orange (Figure 11 d – i)

Lamination Counts

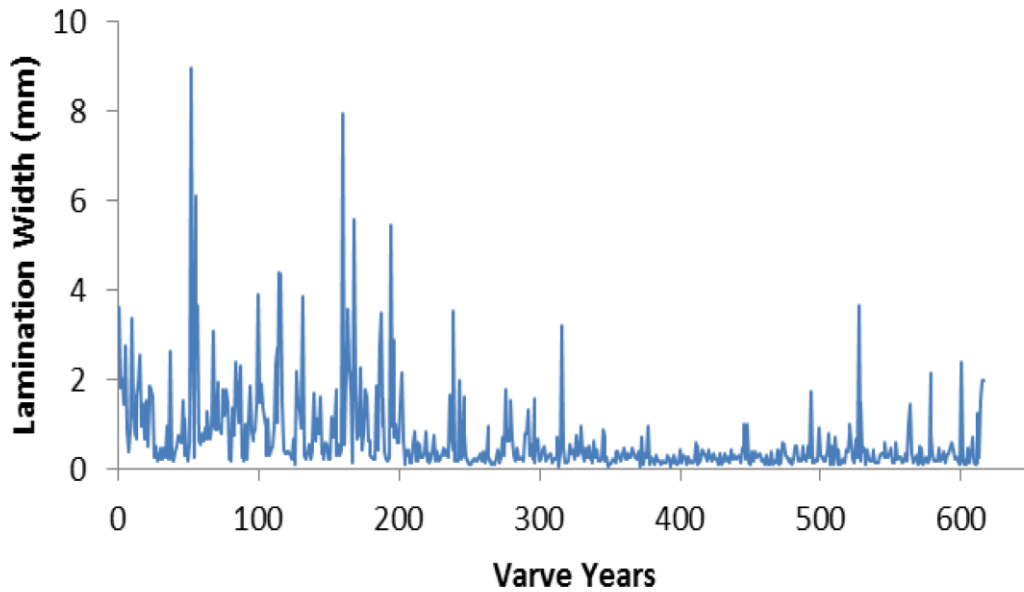
A total of ~ 617 - 621 discontinuous laminations were counted in the upper 50 cm of West Basin Lake sediments and averaged 0.57 mm (0.66 mm true width). However, due to the diffuse nature of most laminations, local zones of deformation and several zones where laminations appear absent (especially between 70 – 140 mm, bar one organic rich lamination), identifying and measuring laminations was mostly very difficult. Due to the difficulty in lamination identification, this likely caused over and/or under estimation of the laminations across the entire core or at least in particular zones.

With increasing depth, laminations generally became thinner (Figure 5). This was expected as older, deeper varves are impacted by overburden. However, lamination

frequency became greater with depth (Figure 5) but was also be accentuated by compaction.

A

Lamination Thickness Variation through Time



B

Lamination Frequency Variation through Depth

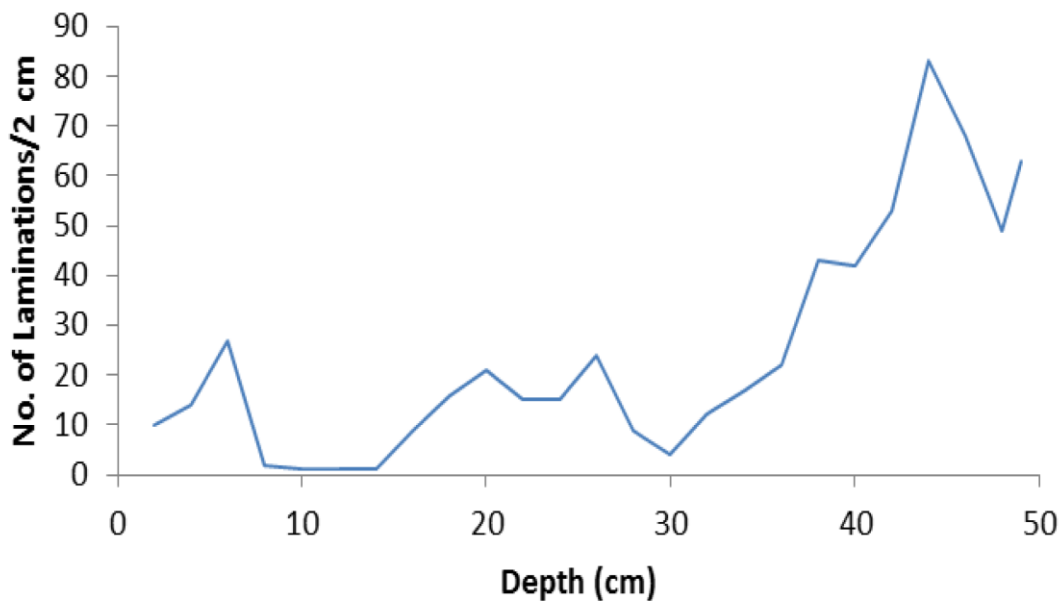


Figure 5: (a) Shows lamination thickness variation through time and an increasing lamination thickness towards present day. This plot does not display thicknesses of zones where laminations appeared absent and hence, splices the laminated zones as a continuous chronology (i.e. the 621st lamination is likely older than 621 years). Thus, is only here to show the trend that lamination widths decrease with age. (b) Shows lamination frequency variation with depth and an increase in lamination frequency per 2 cm with depth. The widths of the laminations have been corrected for shrinkage and represent true widths in both plots.

Depth – Age Relationship

The depth age model reproduced from Gell et al. (1994) and Last and De Deckker (1990) was based on three radiocarbon dates and six independent Pb210 (Figure 6). The cumulative number of laminations per 2 cm, counted in the upper 490 mm of West Basin lake sediments, was plotted over the model and demonstrated a trend closely resembling to that exhibited by the depth-age curve. This suggested there was approximately 617 - 621 years of deposition in the upper 50 cm of West Basin Lake sediment and that the laminations could potentially represent varves. The majority of data from West Basin lied within or at least on the edge of the 95% confidence interval (grey region) and did not deviate significantly from the model curve. However, the data began deviating from the curve around 45 cm and likely reflected an overestimation of laminations counted for the lower portions of the sediment. Please be reminded that this data implied a continuous varve chronology which was not the case for the upper 490 mm of West Basin lake sediments.

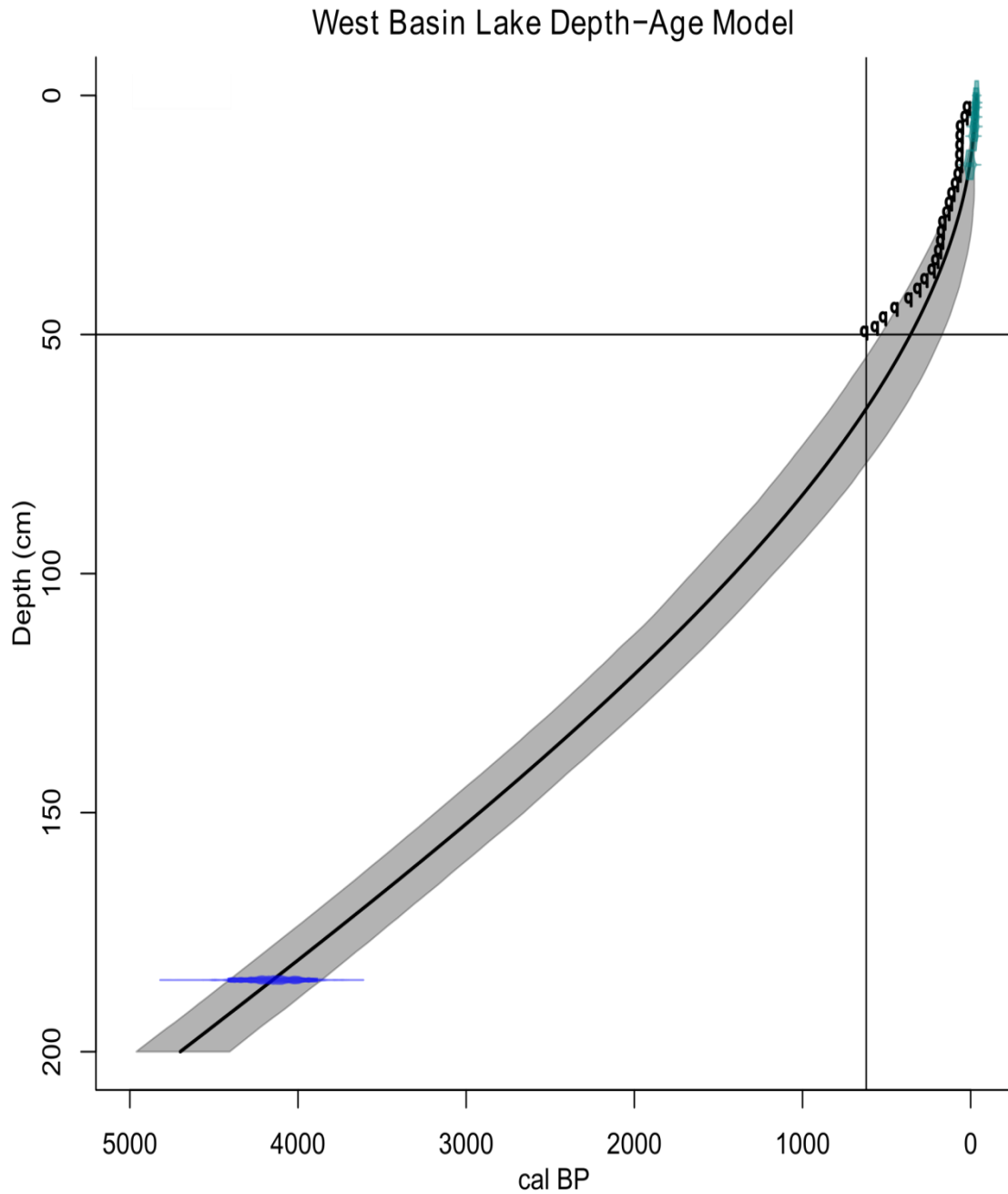


Figure 6: A reproduction of the top of the depth-age model for West Basin Lake adapted from Gell et al. (1994). The form of the curve is a spline. The green data represent six independent Pb210 ages and the blue data represents the earliest of three ¹⁴C radiocarbon age probability density histograms produced from West Basin Lake (Last and De Deckker 1990). The grey band represents the 95% confidence interval. The series of data points (black, open pinpoints) represents the cumulative number of laminations per 2 cm of West Basin Lake sediment. The horizontal and vertical lines intersect at 50 cm depth and 621 cal BP respectively and 0 cal BP = 1986.

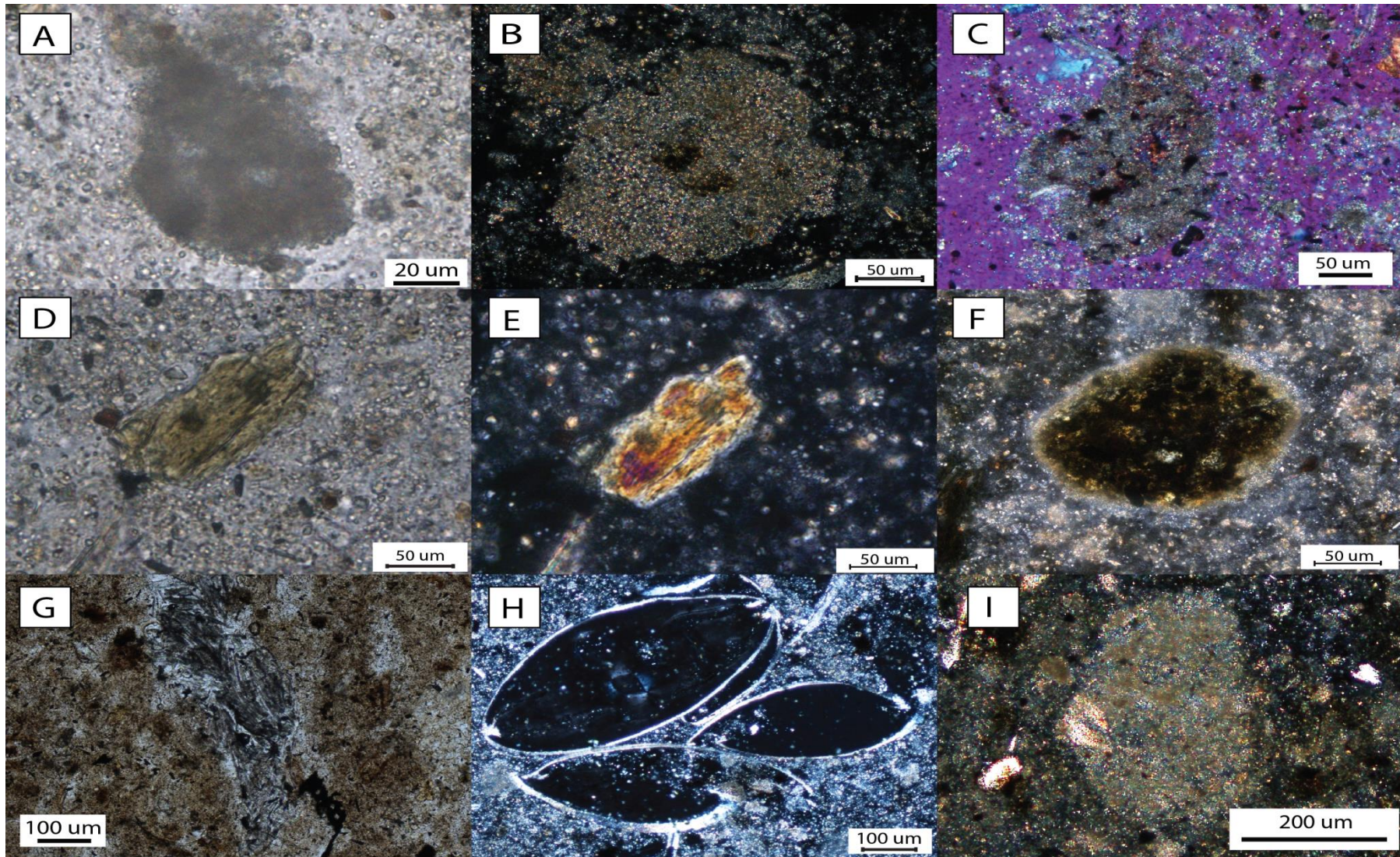


Figure 7: Photomicrographs of some of the common constituents of the calcareous component of West Basin Lake sediments. (a) A typical sub-rounded, sub-spherical peloid of microcrystalline carbonates (micrite) also exhibiting a cloudiness which is not uncommon (PPL). (b) A similar peloid viewed under XPL displaying third order creamy birefringent colours. It also appears to have some organic matter, most obvious in the centre, and probably accounts for the slight brown colouration. (c) A peloid viewed under XPL with the λ 530 nm tint plate inserted, displaying third order birefringent colours giving an overall creamy green appearance. (d) A mineral commonly seen disseminated throughout the profile. Its relief changed upon stage rotation, a common property of carbonate minerals. The brown colouration could be a staining by organic matter, or may be the Fe bearing carbonate, siderite. (e) The same mineral grain viewed under XPL displaying first order orange/yellow birefringent colours. (f) A peloid/intraclast of unknown composition, potentially fecal in origin, sitting in a carbonate rich matrix. Its optical properties were not vastly different between PPL and XPL and may indicate an organic composition represented by the opaque material within it. A thin micritic envelope can also be seen around the grain. (g) A small cluster of acicular, colourless-grey minerals (potentially aragonite or needle-calcite) in an organic rich matrix. Relief changes were observed upon rotation of the stage and exhibited third order creamy birefringence colours under XPL. This crystal habit of carbonates or at least a clustering of them was a rare occurrence. (h) A small cluster of well-articulated ostracod valves in a carbonate rich matrix (XPL). They commonly exhibit a sweeping extinction in XPL (i) A peloid/intraclast of micrite viewed under XPL. Notice the inclusion to the left of centre of the clast which appears to truncate at the grain boundary. This might indicate the clast was already lithified and may originate from the nearshore hardgrounds of the lake. The light brown colouration of the clast and surrounding carbonate matrix probably indicates organic matter is also present.

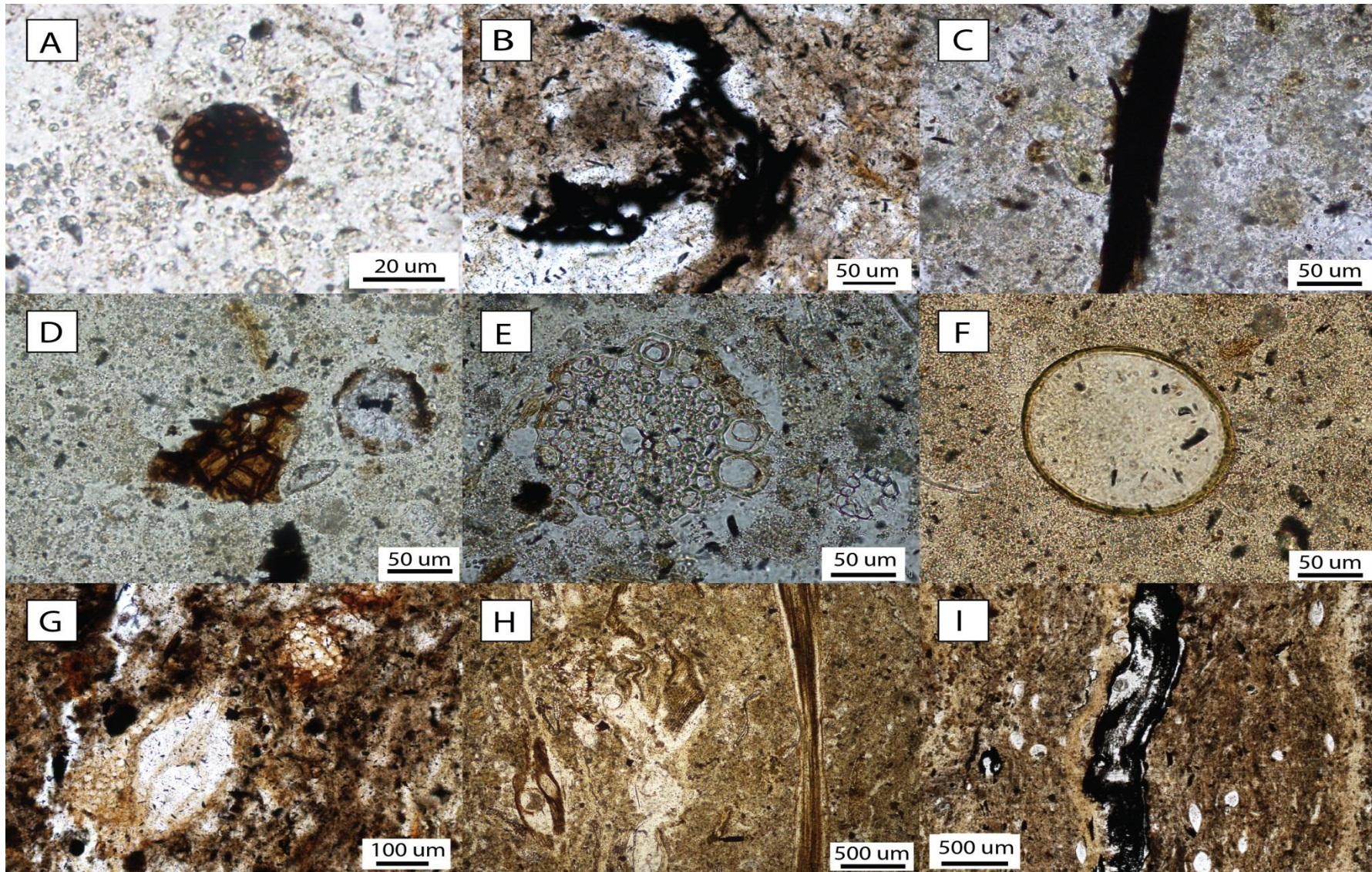


Figure 8: Photomicrographs of some of the common constituents of the organic component of West Basin Lake sediments. All images were acquired in PPL. (a) An organic particle of what may be a pollen spore or other plant component. It appears to have cellular structure. (b) A particle of amorphous organic matter. There is an associated pore space (colourless) which may have once been occupied by more matter which has since disintegrated. (c) A common, more tabular, elongate and larger particle of organic matter. Smaller particles of opaque amorphous organic matter can be seen speckled through the surrounding carbonate matrix. (d) The brown, triangular shaped particle in the centre is an example of another common particle of organic matter which appears translucent and brown - reddish brown in PPL but becomes opaque in XPL. Cellular structure is clearly evident. (e) A transverse image of what might be a vegetative stem. Cellular structure is strikingly prominent. (f) A very common component throughout the sediment. They are morphologically consistent and are likely to be pollen spores. (g) This image captures an organic rich zone, recognisable by the dark brown sediment and disseminated, black amorphous organic matter throughout. The ~ 200 um sized particle slightly left of centre, may represent another transverse through a vegetative stem. Although it is not easily visible at this scale, at higher magnifications, cell walls can be discerned. Another more reddish-brown cellular body can be seen toward the top right of the image. (h) An overview of a zone where the largest organic and cellular, likely vegetative tissues have been deposited. (i) A large amorphous particle of organic matter in a carbonate and organic mixed matrix. This may also represent a particle of charcoal.

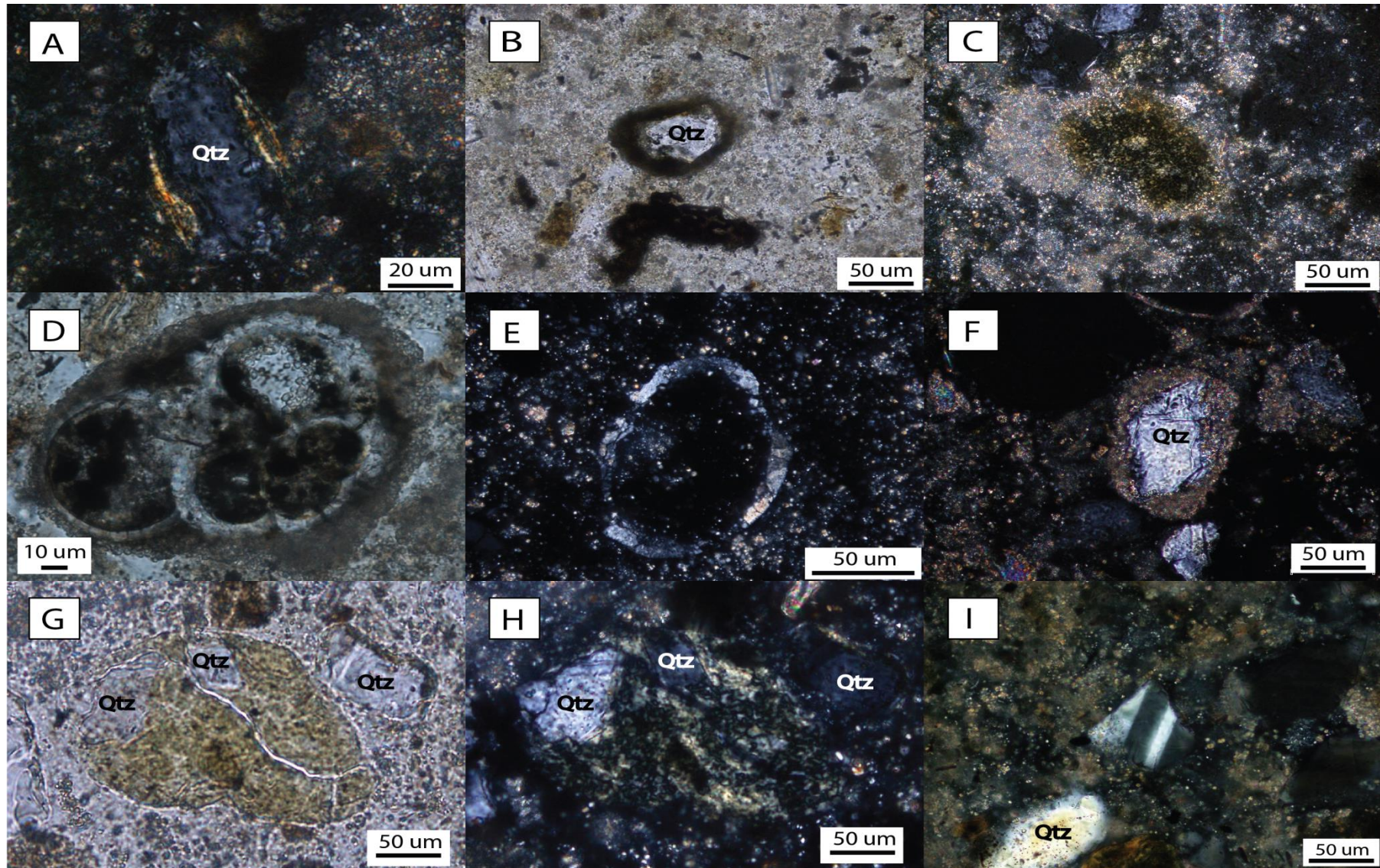


Figure 9: Photomicrographs showing some of the non-carbonate minerals and the nature of grain coatings of West Basin Lake sediments. (a) A mineral grain with the development of a cement coating exhibiting similar third order birefringent orange - yellow colours as the grain in Figure 7 (e). It is not a micritic coating. (b) A mineral grain with a micritic envelope. The micritic envelopes often appear dark – nearly opaque, and hazy. The surrounding matrix is rich in carbonates (note the hazy grey appearance). (c) An XPL image showing a grain exhibiting very low first order yellow birefringence, verging on opaque with an asymmetrical envelope of micrite. (d) A PPL image potentially of the remains of a gastropod. Chambers have been filled with micrite and opaque material which may be organic. In the left most chamber, you can notice a segmentation type pattern in the calcareous wall. Blocky calcite appears to be replacing the original wall of the upper right chamber. A micritic envelope can be seen. (e) An XPL image showing a ghost grain with a rare example of a coating which is not micritic but is most likely calcitic or dolomitic. The original grain appears to have dissolved and micrite has begun filling in the space. (f) An XPL image of a quartz grain with an envelope of micrite. (g) A PPL image of a translucent clast containing smaller grains of quartz. (h) An XPL image of (h). The clast shows a mottled colouration and looks as though it may have undergone some chemical alteration. It may have originated from the nearshore hardgrounds of the lake. (i) An XPL image of a small grain of feldspar, exhibiting multiple twinning. The surrounding carbonate matrix has a brown colouration possibly attributable to the presence of organic matter.

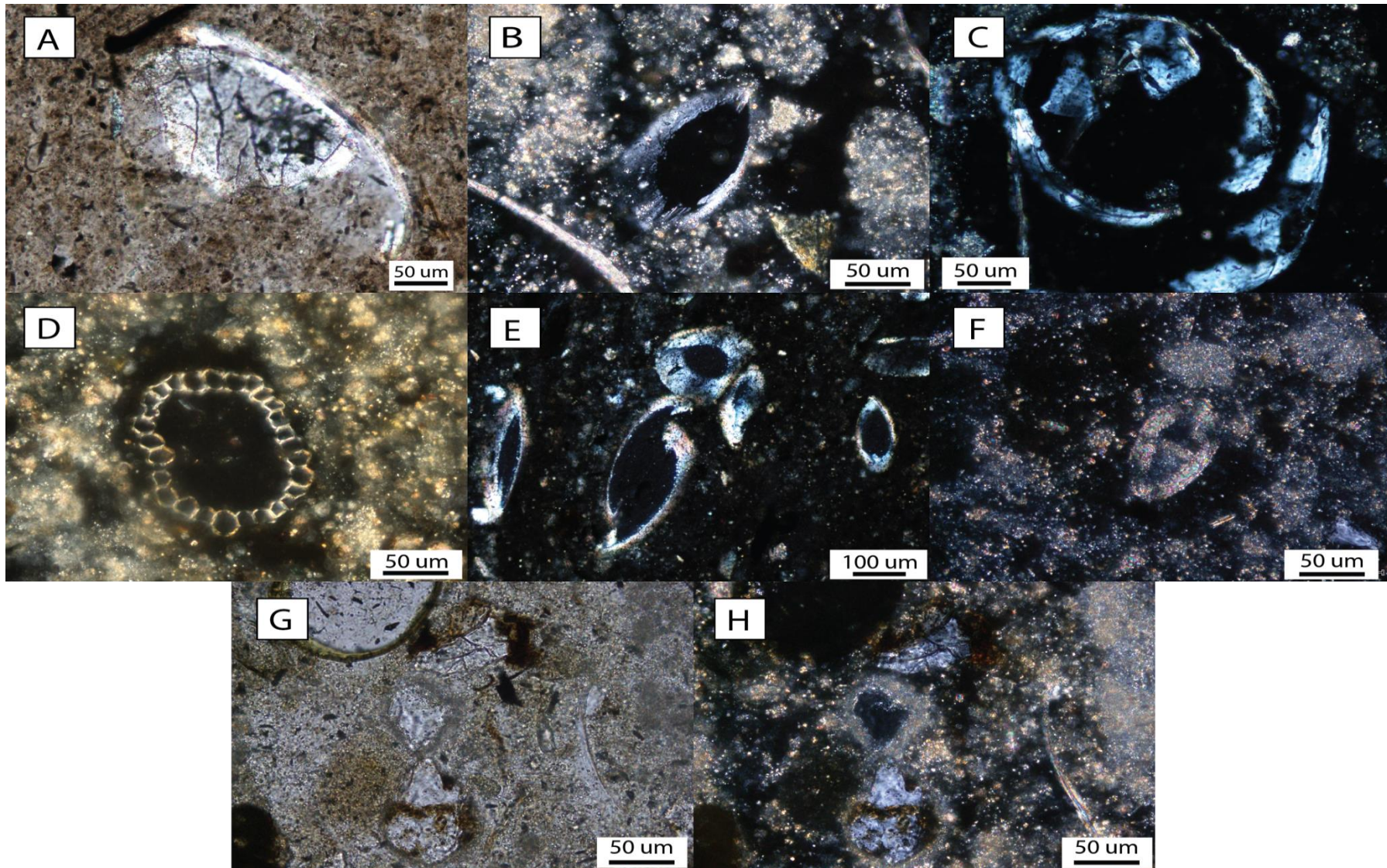


Figure 10: Photomicrographs showing some of the diagenetic mineral precipitation of West basin Lake sediments. (a) A PPL image showing blocky carbonate crystals (likely calcite or dolomite) growing from one half of an ostracod valve. (b) An XPL image of an originally well-articulated ostracod valve appearing to have been replaced by microcrystalline carbonate crystals. The fabric appears fibrous where the two valves meet. (c) A similar XPL image to (b) showing ostracod valves and fragments being replaced by microcrystalline carbonates. (d) An XPL image of vegetative tissue where the cellular structures have been replaced by calcareous cement. (e) An XPL image of more ostracods being replaced by microcrystalline carbonates. Notice the pore space has nearly been completely filled in the top-centre ostracods. The sweeping, cross-extinction can be seen, especially in the above centre ostracod. (f) An apparent growth of calcite forming around an unidentified nucleus (g) A PPL image showing two mineral grains with incomplete coatings of dark reddish-brown cement. Note how it cuts through the lowermost grain. Some relief change was noted in the crystals of the cement in the lowermost grain upon rotation of the stage, indicating it could be a carbonate (siderite). (h) An XPL image of (g). The central grain has a micritic envelope as well as the lowermost grain.

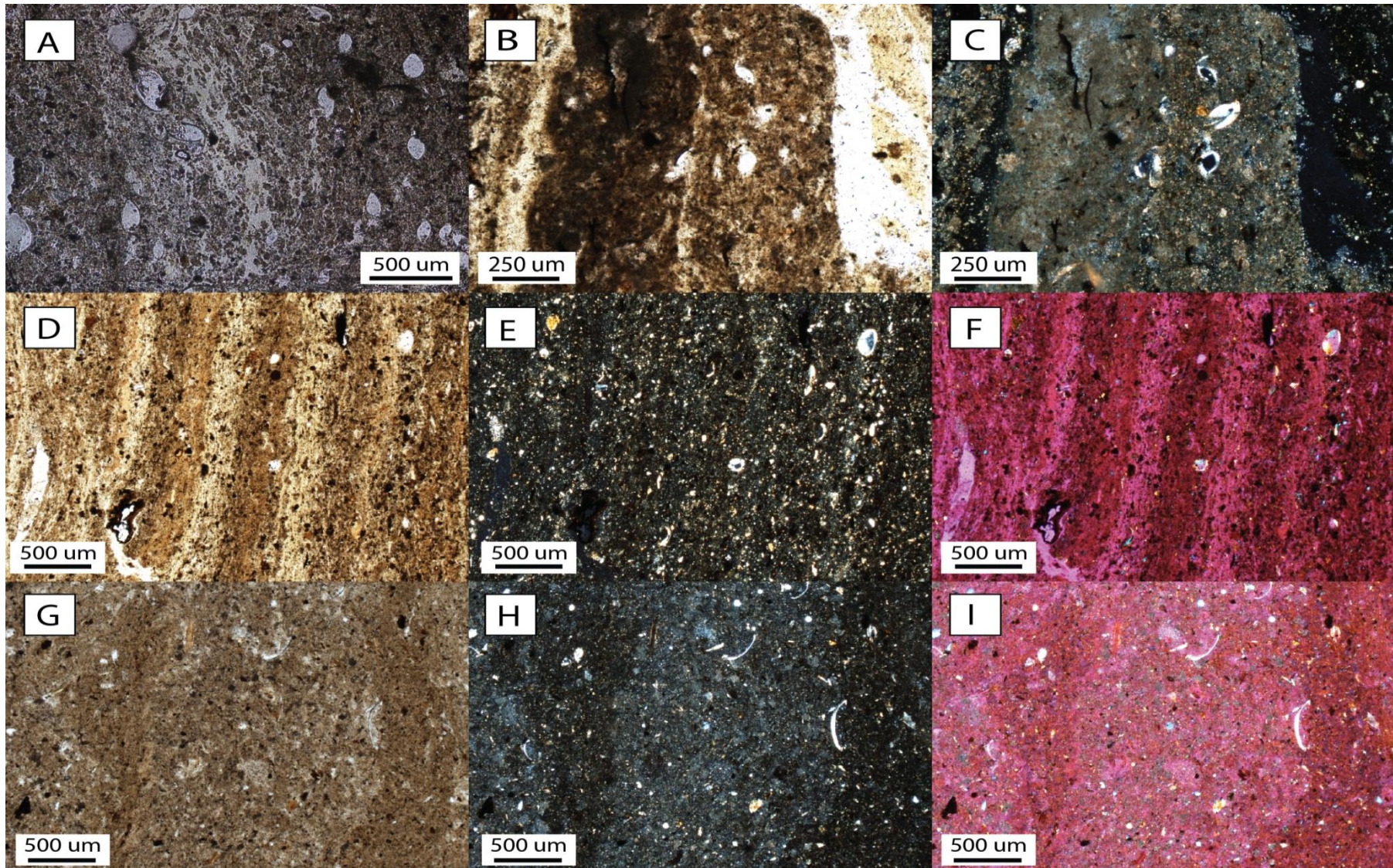


Figure 11: Photomicrographs showing the general characteristics of the laminations in West basin Lake sediments. The top of the core is to the left in all images. (a) A PPL image showing one of the lightest, slightly yellow laminations running sub-vertically through the centre. The adjacent sediment is also quite peloidal. The surrounding sediment either side is carbonate rich. (b) A PPL image showing a thick carbonate lamination also rich in organics, attributing the brown colour. Note the grading of coarser carbonate minerals at the base (right) into finer, more micritic, darker and denser sediment into the top (left). (c) An XPL image of (b) where the difference in coarseness can be more clearly noted. Also note the cloudy appearance of the lamination, characteristic of carbonate rich components. (d – f) Image series of organic rich laminations in PPL, XPL and XPL with the λ 530 nm tint plate inserted respectively. Notice how under XPL, without the tint plate (e), the laminations become much harder to distinguish as organic content remains opaque or becomes darker, creating the illusion of a homogenous sediment. Even the abundant clastics and non-carbonate grains are homogeneously disseminated throughout. The darkest lamina is likely to be the richest in organics, whilst the lightest, slightly yellow appear sparse in any type of component and has mostly become occupied with resin. Notice that there appears to be a repetitive and cyclic deposition. (g – i) Image series of alternating carbonate and organic rich laminations taken under PPL, XPL and XPL + tint plate respectively. Note how the sediment appears nearly homogeneously coloured and composite under PPL (g) but under XPL, without and with the tint plate inserted (h and i respectively), compositionally contrasting laminations are revealed. The XPL image (h) reveals a carbonate rich lamination in the centre, bracketed by darker, nearly opaque organic rich laminations either side. The XPL + tint plate image (i) showcases the diagnostic third order creamy green birefringence of carbonate rich lamina. Note how there is little change in the organic matter between PPL and XPL + tint plate, but sometimes appearing with orange hues as seen in (i).

Scanning electron microscope (SEM) Micro-facies Analysis

Three different modes of the SEM were trialled to determine the best approach for investigating fine scale structures and image acquisition.

LOW VACUUM SEM USING SOFT SEDIMENT

Initially, low vacuum mode was tested using a 70 x 12 x 10 mm block of sediment from East Basin Lake. But after 2 hours, the sample dried out, shrunk, cracked and salt began crystallising on the sediment surface. This severely obscured the sedimentary detail which was difficult to discern to begin with. This mode was also limiting in terms of magnification strength i.e. resolution was weak approaching x5000 magnification and was lost at greater than x10, 000 magnification.

ENVIRONMENTAL SEM (ESEM) USING SOFT SEDIMENT

This method required very small samples (~ 50 x 50 mm cubes) for analysis and therefore imaging continuity of the core was very inefficient. However, this mode enabled fine control of the humidity in the vacuum chamber and was gradually reduced at 10% increments down to 30% humidity. But after an hour, salt crystals formed covering the entirety of the sample surfaces. On a different sample, the humidity was only reduced to 55% but after an hour, some salt crystals still formed on the sediment surfaces and shrinkage still occurred. But keeping the humidity too high (>60%) compromised the image quality. Like the low vacuum mode, ESEM was not the quickest and most efficient method to easily discern compositional contrasts either. However, compositional variations throughout the sediment were rarely abrupt or distinct.

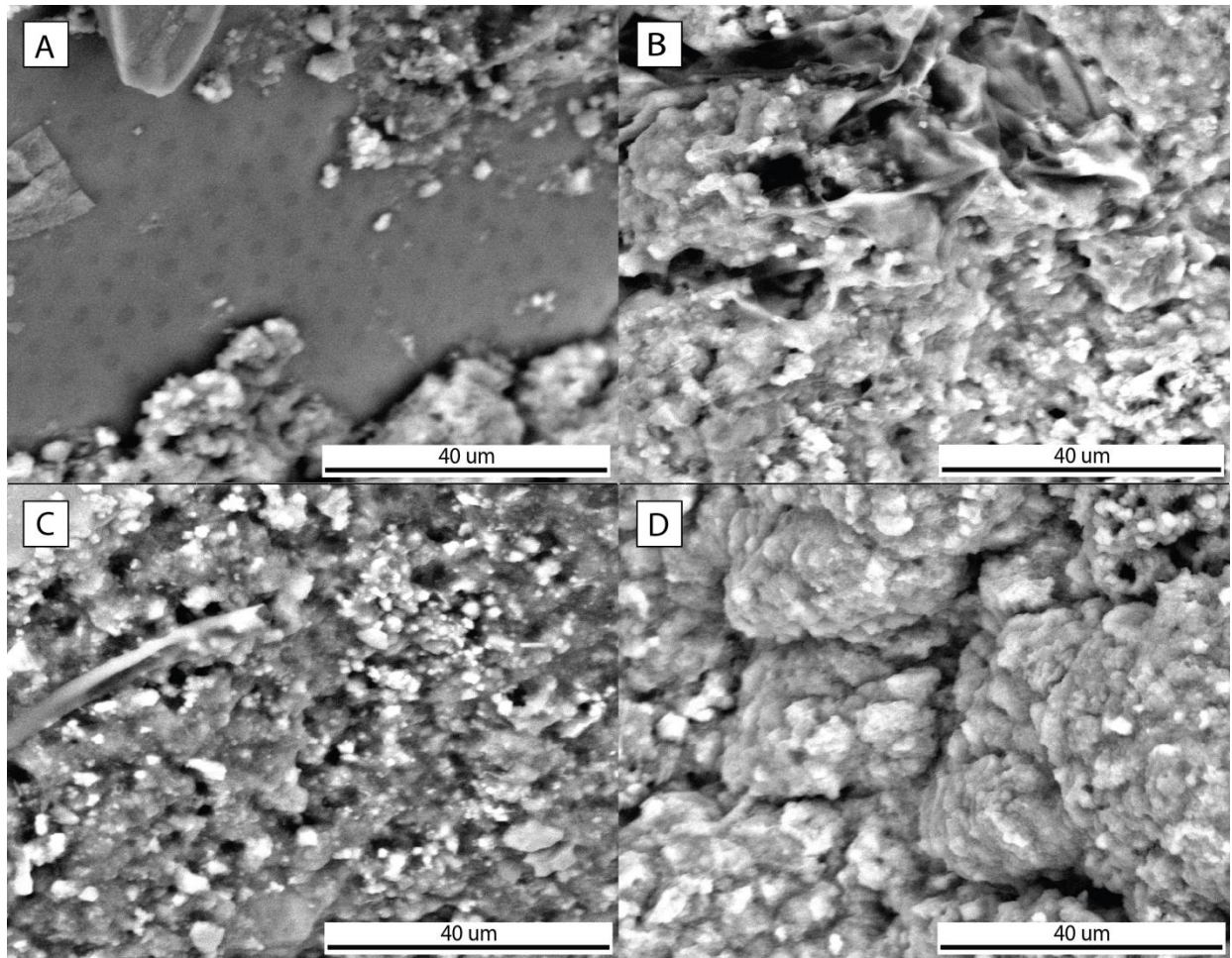


Figure 12: A series of backscatter electron micrographs acquired using ESEM mode, imaging a ~ 50 x 50 x 50 mm cube of raw, wet West Basin Lake sediment extracted between 100 – 110 mm depth from the core. (a) Shows what is likely the surface of an ostracod shell - notice the porous texture. (b) Notice in the top of the image, an amorphous wavy, folded, slightly darker looking particle embedded in the matrix which is likely organic matter. (c) A good representation of the fineness of the carbonate and clay sized non-carbonate grains (bright white particles) embedded in what is probably an organic matrix (darker and grey). (d) Notice the larger, clumpy grains which probably represent the peloid grains commonly observed in thin section of carbonate rich lamina.

HIGH VACUUM SEM USING RESIN EMBEDDED SEDIMENTS

Using this approach was preferable regarding being able to observe structural and compositional detail as the samples had polished surfaces. The samples could be used as a whole and the possibility of obscurity by cracks or salt crystals over time was eliminated. The magnification limits were drastically increased compared to low vacuum and ESEM modes.

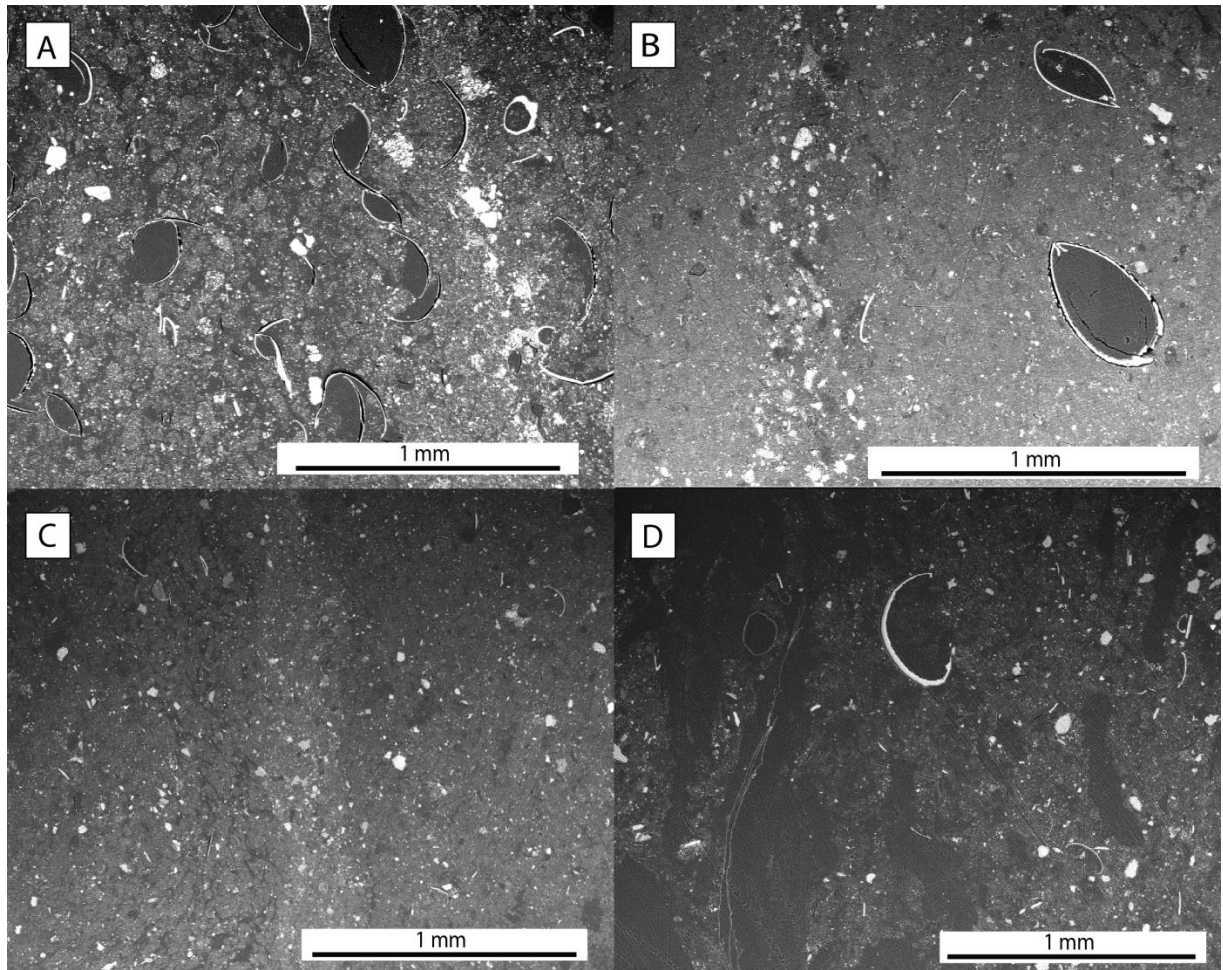


Figure 13: A series of backscatter electron micrographs acquired using high vacuum mode imaging various solid, resin embedded West Basin Lake samples. The top of the core is to the left in all images (a) Notice the abundance of peloidal grains constituting much of the sediment. There is a good degree of intergranular porosity amongst the peloids where dark grey resin has infiltrated. Several ostracods can also be seen and the voids within them have been infiltrated by resin. The more anhedral, broken up bright grains in the right portion of the image are likely to be carbonates and/or purely micritic peloids whereas the more euhedral grains are more likely non-carbonates such as quartz and other silicates. (b) The matrix here is much more dense and homogenised and peloids cannot be recognised. A lamination running vertically, slightly left of centre and is abundant with carbonate and various detrital grains can be distinguished. Two ostracod valves can be seen in the right portion of the image. Some dark grey material is speckled throughout and probably represents organic matter and/or potentially pore space. (c) A thin lamination running vertically through the centre of apparently homogenous looking sediment can be distinguished. It is likely richer in carbonates and/or silicates than the adjacent sediment either side. (d) Notice the large pore spaces which appear to have been completely infiltrated with resin actually also contain large, cellular plant tissue which can no longer be discerned.

Down-core variability in Sediment Composition

The pattern of sedimentation variability through depth reflects predominantly prolonged periods of carbonate deposition vs organic in West Basin Lake. This means that in a zone rich in organic matter, laminations are more often organic upon organic (Figure 11; d –f) and vice versa in carbonate rich zones. However laminations are much more difficult to discern within carbonate rich zones, as they vary much less than the organic zones. This is especially true in the upper 140 mm (thin section depth) carbonate rich sediment where the thickest and least laminations are identified.

DISCUSSION

Are the Laminations Varves?

There is evidence to suggest that the laminations in West Basin Lake are varved but cannot be confidently concluded. The uppermost 50 cm consists of finely laminated, organic-carbonate sediments of a size and frequency that are typically associated with varved lake sediments. Varves hold tremendous potential as palaeoclimate indicators, allowing for the development of precise chronologies and annual scale climate reconstructions. To date, no Holocene varve sequence has been identified in Australia (Walker and Owen 1999, Neukom and Gergis 2012) thus the sediment record from West Basin Lake is particularly interesting. However, before any palaeoclimate information can be extracted from the West Basin record, a more detailed assessment as to whether or not the sediments are indeed varves is required. Through micro-facies analysis of the West Basin lake sediments, this ‘varve hypothesis’ can be examined using two tests. Test one relates to the physical and chemical composition of the West Basin lake laminations, coupled with an understanding of the modern day lake

environment: is the nature of the sediment laminations and the conditions in the modern lake, conducive to a varve deposition hypothesis? Test two encompasses the physical data including lamination frequency and radiometric depth-age modelling: does the number of laminations at West Basin comply with an independent estimate of sediment age? These two tests will be evaluated through the following discussion.

POTENTIAL FOR VARVE DEPOSITION

The proliferation of life forms, physical and chemical processes operating within and around a lake and the subsequent sediment yield are all strongly influenced by seasonal forcing (Brauer 2004, Zolitschka 2007). According to (Zolitschka 2007), overall climatic conditions and more importantly, seasonal variability, will govern varved sediment formation in a lake more than long-term climate variability of half the amplitude.

Weather data obtained from the Australian Bureau of Meteorology (BOM 2014) web page recorded at the Colac shire station, Colac, Victoria, indicate seasonal cycles in mean monthly maximum temperature and rainfall (Figure 14) and so, it is expected that seasonal components comprising a varve will be reflected in the lake sediments of West Basin.

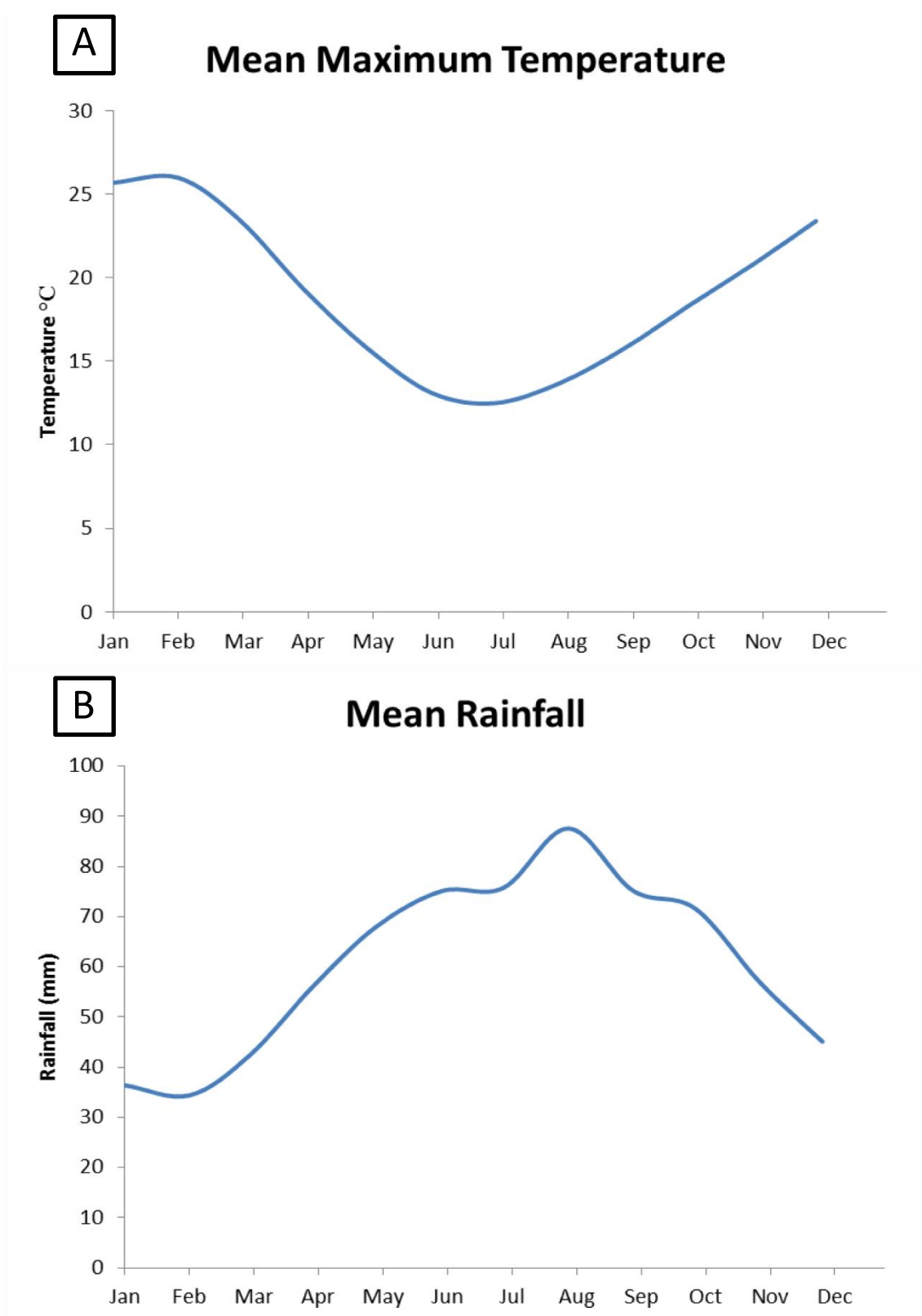


Figure 14: (a) shows mean monthly maximum temperature during the period 1899 – 1983 for the Colac region, Victoria. (b) shows mean monthly rainfall during the period 1898 – 2014 for the Colac region, Victoria.

CARBONATE VS. ORGANIC DEPOSITION

The composition of West Basin lake sediments clearly contains seasonally distinct materials – carbonates (summer precipitates), plus organics (spring/autumn biogenic detritus). According to (Gell et al. 1994), endogenic carbonates (mainly dolomite, calcite, hydromagnesite and magnesite), organic matter, detrital feldspars, clay minerals, quartz and ferromagnesian minerals make up the modern off-shore sediments.

Dissolved inorganic carbon solubility is dependent on lake water pH and if the water column becomes saturated with CO_3^- , usually beyond pH 8, CaCO_3 can begin to precipitate (O'Sullivan 1983). In the case of West Basin Lake, the pH of the monimolimnion is 8.9 while the mixolimnion is slightly higher at 9.0 and the entire water column of West Basin lake is supersaturated with respect to calcite, aragonite, dolomite, magnesite and hydromagnesite (Last and De Deckker 1990). The high Mg/Ca ratio in West Basin lake is favourable for dolomite and hydromagnesite formation, rather than the more common occurrences of calcite or aragonite seen for many other lacustrine settings (Last and De Deckker 1990). Both low-Mg calcite and aragonite have biogenetic carbonate shell material origins, whilst most other carbonate material is believed to be endogenic, precipitating within the water column of the lake (Last and De Deckker 1990).

Calcium carbonate precipitation occurs in summer, favoured by high productivity and warm water conditions (Brunskill 1969, Wittkop et al. 2009) exhibited by Fayetteville Green Lake, New York (Brunskill 1969). Fayetteville Green lake is meromictic with lamina classified as annual couplets resulting from seasonal sedimentation of calcite,

greatest during the summer, with deposition of organic matter throughout the year (Brunskill 1969).

However, endogenic carbonate minerals occur throughout the entire 50 cm of studied sediment and thus indicate its presence is not exclusively seasonal. It suggests the lake water has been alkaline and actively precipitating carbonates during most of the lake's Holocene history (Last and De Deckker 1990, Gell et al. 1994).

POTENTIAL FOR VARVE PRESERVATION

Volcanic crater (maar) lakes, such as West Basin, are favourable for varve preservation as they tend to be deep, morphologically sheltered and undisturbed by wind (Brauer 2004). However, distinctly different morphometric and catchment settings have been shown to successfully preserve seasonal laminations as evidenced by two north east German lakes (Kienel et al. 2013) and should not be relied upon as a rule of thumb for varve deposition and preservation.

West Basin Meromixis and Anoxia

In non-glaciated lakes, almost all varved sediments are exclusively found in meromictic lakes (O'Sullivan 1983). Meromixis is a phenomenon in which layers of water become stratified, forming a monimolimnion (lower body) and mixolimnion (upper body) which thereafter, do not mix.

Timms (1972) attributed the onset of meromixis in West basin to western Victoria's recent history of extended drought and times of excessive rainfall. Several severe droughts and flooding events occurred during the 1900's and meromixis may have

established sometime around 1968 (Timms 1972). In conjunction, West Basins' abrupt and steep 20 – 35 m high crater walls, protecting it from wind disturbance, likely facilitated meromixis establishment (Timms 1972). In West basin, the monimolimnion is anoxic and more saline than the above mixolimnion (Last and De Deckker 1990).

Kienel et al. (2013) attributed varve preservation in two north east German lakes to an anoxic monimolimnion as a result of organic matter accumulation, facilitated by a reduction of lake circulation intensity and increased nutrient input from nearby agricultural establishments, further promoting organic matter production. A similar meromictic nature at West Basin lake should therefore imply that varve preventative processes such as bioturbation, wind or density-driven lake water circulation and bottom currents (Zolitschka 2007) are not effectual to a great extent.

Why not Varves?

Although temperature and precipitation of the recent century demonstrate seasonal fluctuations, seasonal cyclicity or repetition of alternating lamination types was not clearly defined and pervasive in the upper West Basin Lake sediments. In zones where the laminations were unapparent or completely absent (especially the entire 70 – 140 mm interval), could indicate a destabilisation of lake meromixis. If lake level falls below a critical point, meromixis will destabilise and cease the formation of varves (Lowe et al. 1997). Gouramanis et al. (2013) suggested meromixis would not persist in West Basin lake.

The occurrence of framboidal pyrite (Figure 4) implies that microbial reduction of sulphate dissolved in pore waters may be governing H_2S (or HS^-) and HCO_3^-

production according to: $2\text{FeOOH} + \text{CH}_2\text{O} + 3\text{SO}_4^{2-} \rightarrow 6\text{HCO}_3^- + \text{FeS} + \text{FeS}_2 + 4\text{H}_2\text{O}$ (Dedeckker and Last 1988). This would increase alkalinity and be conducive to authigenic precipitation of carbonate minerals in the pore space (Last and De Deckker 1990). If meromixis was destabilised and mixing and potential oxygenation of the sediment-water interface was allowed, then the formation of sulphuric acid (H_2SO_4) may reduce lake pH enough to cause carbonate dissolution and explain the observed hiatuses in carbonate laminations.

Alternatively, if methanogenic bacteria have an instrumental role in establishing or maintaining alkalinity at the sediment water interface or in the anaerobic pore water according to: $\text{CO}_2 + 8\text{H} \rightarrow \text{CH}_4 + 2\text{H}_2\text{O}$ (Last and De Deckker 1990) and meromixis was disestablished, oxygenation would terminate this process and therefore decrease alkalinity at the sediment water interface and cause termination of carbonate precipitation and varve preservation.

DEPTH-AGE RELATIONSHIP

The comparison between radiometric and lamination number (Figure 6) provides some ammunition in support of an annual nature of deposition of the laminations. However, there are a number of uncertainties that must be taken into account when making this comparison. Firstly the laminations within the 50 cm of studied sediment are not continuous and become interrupted by several zones where laminations appear absent (Figure 15). Part of this absence may relate to technical limitations, i.e. laminations may have been unable to be distinguished by optical microscopy. However, it is also clear that a number of disturbances have taken place within the West basin catchment over the last 100 years, which in turn manifest as marked changes in sediment character. For

example, periods of enhanced organic matter deposition, particularly the non-laminated section between 125 – 130 mm which contains abundant grassy plant remains, is most likely the result of post-European agricultural activity. The period of time associated with such sediment deposition is highly uncertain, thus the comparison between radiometric and lamination counted age also carries uncertainty.



Figure 15: The 70 – 140 mm carbonate rich zone where laminations appear absent/on hiatus

Uncertainties also lie with the radiocarbon age model. The depth-age curve is constructed based on only three ^{14}C radiocarbon dates (see Last and De Deckker (1990) and six independent Pb210 dates restricted within the top 15 cm of sediment (Figure 5). Radiocarbon dating is a generally imprecise dating technique as ^{14}C has varied non-constantly over time and therefore one ^{14}C year will not equate to one calendar year (Jellison and Melack 1988). Radiocarbon dates therefore require calibration against the radiocarbon calibration curve to be transformed to absolute ages (Jellison and Melack 1988). The output after calibration is a probability density function (Figure 5) within which the absolute age lies and can never be pinpointed precisely. If the radiocarbon date calibrates to a radiocarbon plateau in the calibration curve, very broad density distributions arise and the absolute age becomes much more uncertain (Brauer 2004). Brauer (2004) found that fashioning depth-age relationships from simulated radiocarbon dates on varved sediments challenges the validity of depth-age modelling techniques. They concluded that no model (linear interpolation, splines etc.) can sensibly perform with only a few dates (Brauer 2004).

Due to these reasons, the age model does not represent accurate or reliable ages for the upper 490 mm of sediment, just mere estimation at best. Furthermore, the discontinuity of these potential varves makes comparisons between the predicted varve age and the radiometric age extremely problematic. Nevertheless, for the most part, the lamination-counted age model falls within the margins of error of the radiometric age model and thus there is no conclusive evidence that the laminations are not varved. Coupled with the understanding of the modern lake system at West basin, it would seem that the laminations are more likely varves than not.

Future Direction

When laminations were counted, it was purely done so through micrographic imagery and was limited to the aspect ratio of the image (i.e. only a small aspect of the sediment was captured in an image for counting). Therefore, laminations which were apparent in the micrographs may not have been laterally extensive across the entire sample/core and may not truly represent a lamination, thus causing potential overestimation. Due to the fineness of the laminations, it was not possible to count by naked eye.

SEM (WHAT ELSE CAN THIS PROVIDE?)

Environmental SEM is very useful for 3D imaging of sediment morphology and textural differences which would be expected to occur between compositionally differing lamina (Figure 11 a – d). But it is important to begin with transmission and reflective optical microscopy to gain as best an insight as possible about the sediment before diving into SEM. If water content of the sediment is high and of hypersaline chemistry, such as the case with West Basin Lake, the raw samples will dry out, shrink, deform and become

obscured by salt crystals. Therefore it is wise to be selective when sampling. An understanding or expectation of what might constitute the sample is important so as not to prolong desiccation and subsequent deformation and obscurities permanently destroying the sample during SEM analysis.

High vacuum SEM is another useful study tool as it highlights compositional variances, though in the case of West Basin lake, variances were not so distinct (Figure 12; a - d).

LA-ICP-MS

Laser ablation inductively coupled plasma mass spectrometry was explored in this study however, due to time constraints and initially problematic data it was unable to be applied. High resolution geochemistry, either using LA-ICP-MS or micro-XRF scanning should be used to relate the fine detailed petrology to the whole core geochemistry and environmental interpretations.

DATING

Further radiocarbon dating of the lake sediments should also be an important future consideration. To date only, three radiocarbon dates have come from West Basin Lake (Last and De Deckker 1990, Gell et al. 1994) and were dated on bulk carbon. Therefore, if old carbon was in the system, it could skew the ages, seemingly making carbon components appear older than they really were. Brauer (2004) indicate that a well dated Holocene section typically should have at least twelve radiocarbon dates.

The dating range across the core should also be extended to better verify a varve chronology and verify with at least another independent dating method (Ojala et al. 2012)

SEDIMENT TRAP STUDIES

It would be wise to compare sediment accumulation rate with that suggested by Pb210 dating and see if there is an agreement as was confirmed in Sugan Lake, China (Zhou et al. 2007). Sediment accumulation trap studies would also confirm endogenic precipitation of carbonates.

CONCLUSIONS

The purpose of this study is to investigate the potential that West Basin lake sediments represent a continuous Holocene varve record. There is evidence to suggest that the sediments are varves and is investigated by two tests. Test one examines the physical and chemical composition of the West Basin lake laminations and if modern lake conditions are conducive to a varve deposition hypothesis. The second test examines the physical data including lamination frequency and radiometric depth-age modelling: does the number of laminations at West Basin comply with an independent estimate of sediment age?

The morphometric, shielded, meromictic and anoxic sediment water interface of West Basin lake is highly conducive to varve preservation and there is good agreement between the number of laminations and an independent estimate of sediment age to imply the laminations are annual. However, through petrographic analyses, seasonal sub-laminae materials constituting a varve, are not easily identifiable or show a repeated, cyclic pattern. Hiatuses where laminations appear absent commonly occur throughout the profile and based on the scope of this study, do not represent a continuous varve record. This does not mean to imply varves are not there, but further warrant for investigation should be pursued in the forms of; thorough SEM and

geochemical analyses, sediment trap studies, regional cross correlative studies between adjacent lakes and more improved dating techniques to better validate varved sediment.

ACKNOWLEDGMENTS

First and foremost, I would like to thank Dr. Jonathan Tyler, my supervisor, my friend and excellent teacher for all his support, guidance and patience throughout the honours year. Thank you to my co. supervisors John Tibby and Cameron Barr for offering their guidance and interest in my project. Thank you to Dr. Katie Howard and Dr. Rosalind King for being great support mentors. Thank you to the staff of Adelaide Microscopy but especially Ruth Williams of Adelaide Microscopy for assisting me and guiding me with resin embedding procedures. Thank you to Aoife McFadden for assistance with LA-ICP-MS data acquisition and processing.

REFERENCES

- 2014 BUREAU OF METEOROLOGY. O. M. Climate data online.
<<http://www.bom.gov.au/climate/data/index.shtml>>.
- BAGNATO S., LINSLEY B. K., HOWE S. S., WELLINGTON G. M. & SALINGER J. 2004 Evaluating the use of the massive coral *Diploastrea heliopora* for paleoclimate reconstruction, *Paleoceanography*, **19**, p.PA1032.
- BARR C., TIBBY J., MARSHALL J. C., MCGREGOR G. B., MOSS P. T., HALVERSON G. P. & FLUIN J. 2013 Combining monitoring, models and palaeolimnology to assess ecosystem response to environmental change at monthly to millennial timescales: the stability of Blue Lake, North Stradbroke Island, Australia, *Freshwater Biology*, **58**, 1614-1630.
- BARR C., TIBBY J., GELL P., TYLER J., ZAWADZKI A. & JACOBSEN G. E. 2014 Climate variability in south-eastern Australia over the last 1500 years inferred from the high-resolution diatom records of two crater lakes, *Quaternary Science Reviews*, **95**, 115-131.
- BOENING C., WILLIS J. K., LANDERER F. W., NEREM R. S. & FASULLO J. 2012 The 2011 La Niña: So strong, the oceans fell, *Geophysical Research Letters*, **39**, p.L19602.
- BRADBURY J. P. & DEAN W. E. 1993 Elk Lake, Minnesota: Evidence for Rapid Climate Change in the North-Central United States : 1993. Geological Society of America, Incorporated.
- BRAUER A. 2004 Annually Laminated Lake Sediments and Their Palaeoclimatic Relevance. In FISCHER H., *et al.* eds. *The Climate in Historical Times*. pp. 109-127. Springer Berlin Heidelberg,
- BRUNSKILL G. J. 1969 Fayetteville Green Lake, New York. II. Precipitation and Sedimentation of Calcite in a Meromictic Lake with Laminated Sediments, *Limnology and Oceanography*, **14**, 830-847.

- COOK E., BUCKLEY B., D'ARRIGO R. & PETERSON M. 2000 Warm-season temperatures since 1600 BC reconstructed from Tasmanian tree rings and their relationship to large-scale sea surface temperature anomalies, *Climate Dynamics*, **16**, 79-91.
- DEDECKKER P. & LAST W. M. 1988 MODERN DOLOMITE DEPOSITION IN CONTINENTAL, SALINE LAKES, WESTERN VICTORIA, AUSTRALIA, *Geology*, **16**, 29-32.
- FOWLER A. M. 2008 ENSO history recorded in *Agathis australis* (kauri) tree rings. Part B: 423 years of ENSO robustness, *International Journal of Climatology*, **28**, 21-35.
- GELL P., BARKER P., DECKKER P., LAST W. & JELICIC L. 1994 The Holocene history of West Basin Lake, Victoria, Australia; chemical changes based on fossil biota and sediment mineralogy, *Journal of Paleolimnology*, **12**, 235-258.
- GOURAMANIS C., WILKINS D. & DE DECKKER P. 2010 6000 years of environmental changes recorded in Blue Lake, South Australia, based on ostracod ecology and valve chemistry, *Palaeogeography, Palaeoclimatology, Palaeoecology*, **297**, 223-237.
- GOURAMANIS C., DE DECKKER P., SWITZER A. D. & WILKINS D. 2013 Cross-continent comparison of high-resolution Holocene climate records from southern Australia — Deciphering the impacts of far-field teleconnections, *Earth-Science Reviews*, **121**, 55-72.
- JELLISON R. & MELACK J. 1988 Photosynthetic activity of phytoplankton and its relation to environmental factors in hypersaline Mono Lake, California. In MELACK J. ed. *Saline Lakes*. pp. 69-88. Springer Netherlands,
- KIENEL U., DULSKI P., OTT F., LORENZ S. & BRAUER A. 2013 Recently induced anoxia leading to the preservation of seasonal laminae in two NE-German lakes, *Journal of Paleolimnology*, **50**, 535-544.
- KITAGAWA H. & VAN DER PLICHT J. 1998 A 40,000-year varve chronology from Lake Suigetsu, Japan; extension of the (super 14) C calibration curve, *Radiocarbon*, **40**, 505-515.
- LAMOUREUX S. 1994 Embedding unfrozen lake sediments for thin section preparation, *Journal of Paleolimnology*, **10**, 141-146.
- LAMOUREUX S. F. & BRADLEY R. S. 1996 A late Holocene varved sediment record of environmental change from northern Ellesmere Island, Canada, *Journal of Paleolimnology*, **16**, 239-255.
- LANDMANN G., REIMER A., LEMCKE G. & KEMPE S. 1996 Dating Late Glacial abrupt climate changes in the 14,570 yr long continuous varve record of Lake Van, Turkey, *Palaeogeography, Palaeoclimatology, Palaeoecology*, **122**, 107-118.
- LAST W. M. & DE DECKKER P. 1990 Modern and Holocene carbonate sedimentology of two saline volcanic maar lakes, southern Australia, *Sedimentology*, **37**, p.967.
- LOTTER A. F. & LEMCKE G. 1999 Methods for preparing and counting biochemical varves, *Boreas*, **28**, 243-252.
- LOWE D. J., GREEN J. D., NORTHCOTE T. G. & HALL K. J. 1997 Holocene Fluctuations of a Meromictic Lake in Southern British Columbia, *Quaternary Research*, **48**, 100-113.

- NEUKOM R. & GERGIS J. 2012 Southern Hemisphere high-resolution palaeoclimate records of the last 2000 years, *Holocene*, **22**, 501-524.
- O'SULLIVAN P. E. 1983 Annually-laminated lake sediments and the study of Quaternary environmental changes — a review, *Quaternary Science Reviews*, **1**, 245-313.
- OJALA A. E. K., FRANCUS P., ZOLITSCHKA B., BESONEN M. & LAMOUREUX S. F. 2012 Characteristics of sedimentary varve chronologies – A review, *Quaternary Science Reviews*, **43**, 45-60.
- PIKE J. & KEMP A. E. S. 1996 Preparation and analysis techniques for studies of laminated sediments, *Geological Society, London, Special Publications*, **116**, 37-48.
- SHANAHAN T., OVERPECK J., BECK J. W., WHEELER C. W., PECK J., KING J. & SCHOLZ C. 2008 The formation of biogeochemical laminations in Lake Bosumtwi, Ghana, and their usefulness as indicators of past environmental changes, *Journal of Paleolimnology*, **40**, 339-355.
- TIMMS B. V. 1972 A Meromictic Lake in Australia, *Limnology and Oceanography*, **17**, 918-922.
- UMMENHOFER C. C., ENGLAND M. H., MCINTOSH P. C., MEYERS G. A., POOK M. J., RISBEY J. S., GUPTA A. S. & TASCHETTO A. S. 2009 What causes southeast Australia's worst droughts?, *Geophysical Research Letters*, **36**, p.L04706.
- WALKER D. & OWEN J. A. K. 1999 The characteristics and source of laminated mud at Lake Barrine, Northeast Australia, *Quaternary Science Reviews*, **18**, 1597-1624.
- WITTKOP C. A., TERANES J. L., DEAN W. E. & GUILDERTSON T. P. 2009 A lacustrine carbonate record of Holocene seasonality and climate, *Geology*, **37**, 695-698.
- ZHOU A., CHEN F., QIANG M., YANG M. & ZHANG J. 2007 The discovery of annually laminated sediments (varves) from shallow Sugan Lake in inland arid China and their paleoclimatic significance, *Science in China Series D: Earth Sciences*, **50**, 1218-1224.
- ZOLITSCHKA B. 2007 Varved lake sediments, *Encyclopedia of quaternary science*. Elsevier, Amsterdam, 3105-3114.

APPENDIX A: EXTENDED METHODS, RESIN RECIPE & MISC.